Ordering in a frustrated pyrochlore antiferromagnet proximate to a spin liquid

Doron L. Bergman,[1] Gregory A. Fiete,[2] and Leon Balents[1]
[1]*Department of Physics, University of California, Santa Barbara, California 93106-9530, USA*
[2]*Kavli Institute for Theoretical Physics, University of California, Santa Barbara, California 93106-4030, USA*
(Received 8 November 2005; revised manuscript received 13 January 2006; published 3 April 2006)

We perform a general study of spin ordering on the pyrochlore lattice with a 3:1 proportionality of two spin polarizations. Equivalently, this describes valence bond solid conformations of a quantum dimer model on the diamond lattice. We determine the set of likely low-temperature ordered phases, on the assumption that the ordering is weak, i.e., the system is close to a "U(1)" quantum spin liquid in which the 3:1 proportionality is maintained but the spins are strongly fluctuating. The nature of the nine ordered states we find is determined by a "projective symmetry" analysis. All the phases exhibit translational and rotational symmetry breaking, with an enlarged unit cell containing 4–64 primitive cells of the underlying pyrochlore. The simplest of the nine phases is the same "R" state found earlier in a theoretical study of the ordering on the magnetization plateau in the $S=3/2$ materials $CdCr_2O_4$ and $HgCr_2O_4$. We suggest that the spin-dimer model proposed therein undergoes a direct transition from the spin liquid to the R state, and describe a field theory for the universal properties of this critical point, at zero and nonzero temperatures.

DOI: 10.1103/PhysRevB.73.134402 PACS number(s): 75.10.Jm, 64.60.−i, 71.10.−w, 71.27.+a

I. INTRODUCTION

Charge and/or magnetic order is an apparently central feature of the ground states of Mott insulators. The detailed nature of this order can be difficult to understand theoretically, particularly when "frustration" is present. By frustration, we mean the presence of competing interactions, which lead, in some appropriate "classical" limit, to a large number of degenerate ground states. This degeneracy is lifted by fluctuations, thermal and quantum, or additional interactions beyond those of the classical limit. However, the classical degeneracy can be lifted in many different ways, making the ultimate ground state very sensitive to details of the Hamiltonian. Apart from demanding an extremely detailed microscopic understanding of a given material (always desirable, but not so easy to come by), is there any way to attack such problems? The approach we follow in this paper is to presume that fluctuations (in this case quantum) are strong, which requires that the ordering itself is weak (i.e., the charge and/or spin modulations are small in amplitude). If so, we may presume the system to be close to some "liquid" state, in which no order (in the conventional sense—but see below) is present. One may then explore the possible ordered states which occur as weak instabilities of the liquid.

Recently, such a view to *charge* ordered states of two-dimensional lattice boson systems has been systematically pursued in Refs. 1 and 2, with specific precedents in Refs. 3 and 4. In that case, the liquid state was taken to be a superfluid. There, the possible charge ordered Mott insulating states proximate to the superfluid were discussed by considering the instabilities due to proliferation of *vortices*. This was made systematic by uncovering the multiplet structure of the vortex states, determined by symmetry. In particular, vortices were shown to transform under a projective representation of the lattice space group, or projective space/symmetry group (PSG).[36] The PSG was shown to determine the structure of the action of the critical theory for the superfluid-Mott transition, and the nature of the possible charge ordered Mott phases. The PSG depends upon the lattice symmetries (space group) *and* the mean conserved boson density. All the above considerations for bosons apply equally well to spin models with U(1) rather than full SU(2) symmetry, with the conserved S^z taking the role of boson "charge." This situation is not uncommon, as it is realized whenever an approximately isotropic magnet is subjected to a uniform magnetic (Zeeman) field. We will focus on this realization here.

In this paper, we will apply an analogous set of ideas to bosons or spins on the three-dimensional pyrochlore lattice. The pyrochlore lattice, consisting of corner-sharing tetrahedra (Fig. 1), takes a central role in the study of geometrical frustration in three dimensions. A number of materials, in

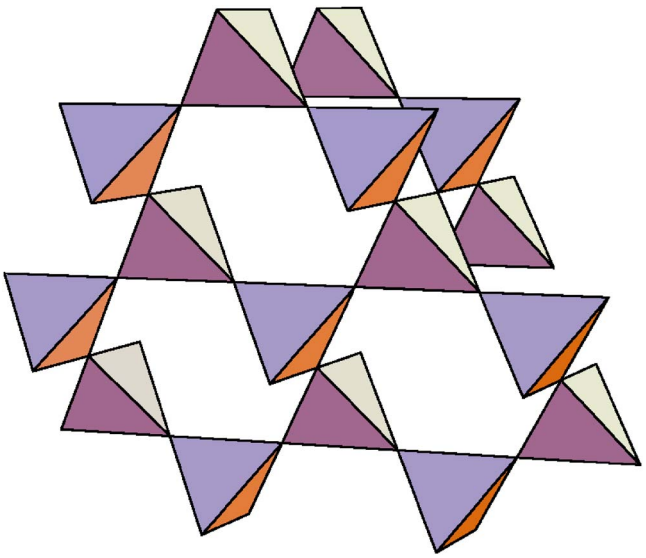

FIG. 1. (Color online) The pyrochlore lattice structures, shown as a network of corner-sharing tetrahedra. The atoms occupy the corners of the teterahedra.

which electronic and/or spin degrees of freedom reside on this lattice, have been intensely studied in this light in recent years. Theoretically, the Heisenberg antiferromagnet on the pyrochlore lattice is interesting as a candidate "spin liquid,"[5,6] in which the fluctuations—thermal or quantum—among frustration-induced degenerate quasi-ground-states prevent the occurrence of long-range magnetic order at temperatures well below the Curie-Weiss temperature, possibly all the way down to $T=0$. Quantum spin liquid states can sustain anomalous spin-1/2 spinon excitations,[7] forbidden in conventional phases of matter.

We therefore choose to take as our proximate liquid phase not a superfluid (or magnetically ordered phase), but instead a particular quantum spin liquid, a so-called "U(1)" spin liquid state (see Ref. 8 and references therein). A general feature (e.g., on different varieties of lattices) of such states is that they exhibit an emergent electromagnetism, i.e., they support an "artificial photon," and excitations can carry emergent U(1) electric and magnetic gauge charges (see Refs. [6,9,10] and references therein). The spinons carry the elementary quanta of the electric charge (of both positive and negative sign in two species of spinon). Another, gapped, topological excitation, a monopole, carries the dual magnetic gauge charge. A transition out of the spin liquid state to a state without broken continuous symmetries is generally described as a condensation of these monopoles. The nature of such a transition, and of the proximate spatially ordered states occurring on the other side of the transition is determined by the monopole PSG. The ingredients determining this PSG, as explored on the cubic lattice in Refs. 11 and 12, are the lattice symmetries and the values of some conserved "background" U(1) gauge charges, which characterize different U(1) liquid states.

To fix these background charges, we will focus on a specific model containing a U(1) spin liquid phase on the pyrochlore lattice. In Ref. 13, this model was argued to describe the physics on the magnetization plateaus observed recently in $CdCr_2O_4$ and $HgCr_2O_4$,[14,15] which are spin-3/2 antiferromagnets with this lattice structure. In particular, the model presumes a local constraint (which may be understood as the restriction to the classical ground state subspace) of three Cr spins fully polarized ($S^z=+3/2$) along the applied field, and another fully polarized antiparallel to it ($S^z=-3/2$), on each tetrahedron.[13,16] We refer to this condition as the "3:1" constraint. The model of Ref. 13 arises as an effective Hamiltonian in this constrained subspace, and takes the approximate form

$$\mathcal{H}_{\mathrm{QDM}} = V\sum_{P} (|\hexagon_A\rangle\langle\hexagon_A| + |\hexagon_B\rangle\langle\hexagon_B|) - K\sum_{P} (|\hexagon_A\rangle\langle\hexagon_B| + \mathrm{H.c.}), \quad (1)$$

where Σ_P indicates a sum over all hexagonal plaquettes on the pyrochlore lattice, and $|\hexagon_A\rangle, |\hexagon_B\rangle$ are specific states with alternating majority and minority spins ($|\uparrow\downarrow\uparrow\downarrow\uparrow\downarrow\rangle$ and $|\downarrow\uparrow\downarrow\uparrow\downarrow\uparrow\rangle$) on the given plaquette. This model is exactly equivalent to a number of other models in the theoretical literature. First, it can be mapped directly to a quantum dimer model on the diamond lattice, the diamond lattice sites being centers of pyrochlore tetrahedra (see Sec. II). A number of such dimer models have been considered in the literature.[17–22] Second, the dimer model in turn can be rewritten as a particular compact U(1) gauge theory. The 3:1 constraint of the spin model maps directly to the background charge of this gauge theory. In this way, the essential ingredients fixing the monopole PSG are determined. A systematic analysis of the spatially ordered states proximate to the spin liquid is therefore possible, and is the main subject pursued in this paper.

More microscopically, it is possible to show that the spin-dimer model of Eq. (1) indeed exhibits a U(1) spin liquid ground state when the dimensionless parameter $v=V/K$ satisfies $v_c<v<1$. This argument, analogous to the ones in Refs. 6 and 22, is described in Sec. II B. The critical coupling v_c is not known, but based on numerical analysis of other similar models probably satisfies $v_c>-0.5$ or so.[20–23] For the application to $CdCr_2O_4$ and $HgCr_2O_4$, it was estimated in Ref. 13 that $v\approx-1.2<v_c$. The nature of the ground state in that case may perhaps be more accurately understood by extrapolation from the limit $v\to-\infty$. The ground state can be determined classically in that limit, and in Ref. 13 was found to exhibit a particular spatial ordering pattern with a quadrupled unit cell. It can be understood by order-by-disorder[24–26] reasoning as the classical state with the most possible "resonances"—off-diagonal quantum moves via the K term in Eq. (1)—with other states. We therefore refer to it as the "R" state.

The alternate approach, which we pursue here, is to approach the physical limit from the spin liquid state, asking which ordering pattern emerges from the PSG analysis. Remarkably, we find that the simplest possible ordered state proximate to the U(1) spin liquid is the R state. This suggests the possibility that the R state in the physical limit may be close to a phase transition to the spin liquid state. The analysis of this paper provides an analytical framework for such a transition, of both quantum and of thermal nature.

Apart from the simplest R state, a number of ordered phases come out of this analysis, and are shown in Figs. 11–19. A salient feature of all these phases is that they exhibit an enlarged unit cell relative to that of the original pyrochlore lattice. Interestingly, this set of phases therefore does not contain the simplest ferrimagnetic ordered state illustrated in Fig. 2, in which the unit cell is not enlarged though the point group symmetry of the crystal is lowered. This indicates that the ground states selected out of the classically degenerate ground state manifold are identifiably different from those preferred by other degeneracy breaking mechanisms, such as, e.g., antiferromagnetic second-neighbor exchange coupling. Identification of the precise nature of the ordered state in experiments therefore indirectly gives useful information on the importance of quantum fluctuations.

The remainder of the paper is organized in the following way. In Sec. II we describe our theoretical model (lattice QED). In Sec. III we illustrate and motivate the dual transformation we make on the Hamiltonian introduced in the previous section. In Sec. IV we derive and present the effective action for the monopole degrees of freedom that appear

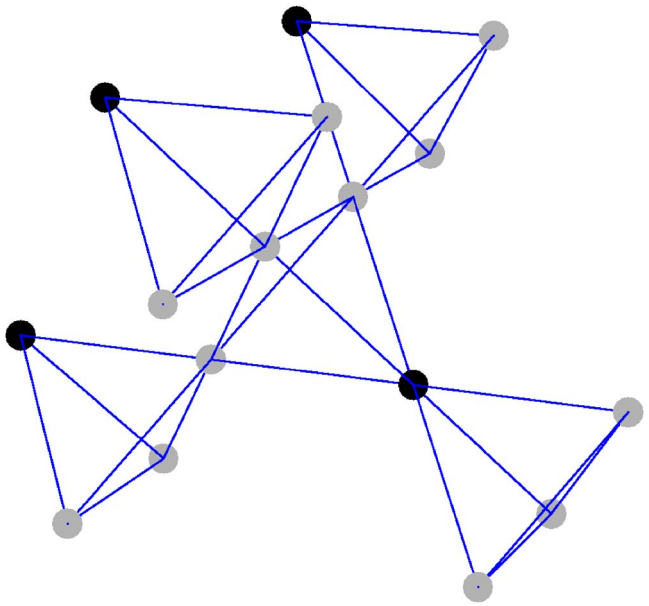

FIG. 2. (Color online) The simplest ordered state consistent with the 3:1 proportion of majority to minority sites, which does *not* exhibit an enlarged unit cell, and has only a fourfold degeneracy. In the spin language, this state has three spins aligned with the field and one antialigned, so we will denote this as a "ferrimagnetic" state, analogous to the ferrimagnetic state found in two-dimensional triangular lattice antiferromagnets in a field. This state is not generically proximate to the U(1) spin liquid.

in the dual theory. We then study the action in the mean-field approximation in Sec. V and present the resulting charge ordered phases in Sec. VI. In Sec. VII we carry out a renormalization group analysis of the action. Finally in Sec. VIII, we conclude with a discussion of the phase diagram and critical phenomena in the spin-dimer model at nonzero temperatures. Important but lengthy formulas and results are given in the Appendixes.

II. THEORETICAL MODEL: FROM SPINS TO COMPACT LATTICE QED

In this section, we reformulate the 3:1 quantum spin-dimer model of Eq. (1) as a lattice U(1) gauge theory, and describe its phase diagram, which contains both spin liquid and ordered states. This Hamiltonian has a single dimensionless parameter $v=V/K$, so the zero-temperature phase diagram is entirely determined by v (we fix $K>0$ by convention—its sign can be changed by a suitable canonical transformation, and has no significance). We discuss the structure of this phase diagram.

A. Equivalence to compact lattice QED

First, it is useful to discuss how the model can be cast into a lattice U(1) gauge theory. A reader not familiar with lattice QED may wish to consult the review by Kogut.[27] As mentioned in the Introduction, it is first convenient to pass from the pyrochlore to the diamond lattice. This is accomplished by focusing on the centers of the tetrahedra (labeled by the sites a and b in Fig. 3) that make up the pyrochlore. The centers of these tetrahedra make up a diamond lattice. Each site on the pyrochlore lattice connects two nearest neighbor tetrahedra, and can be identified with a link between the centers of the two tetrahedra. Thinking in terms of the centers of the tetrahedra as the sites of a new lattice, the spins sit on the links of a diamond lattice. The spin states may therefore be regarded as dimer coverings of the links of the diamond lattice, and the effective Hamiltonian as a quantum dimer model.

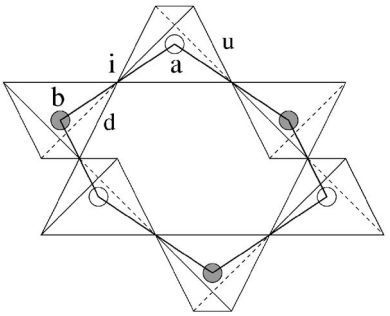

FIG. 3. Section of a pyrochlore lattice. The pyrochlore sites are denoted by i and the tetrahedra are identified by a,b labels. Drawing links between the tetrahedron centers forms the links of a diamond lattice, with the tetrahedron centers corresponding to the sites of the diamond lattice. The figure indicates the bipartite nature of the diamond lattice, which is evident in the notion of up (down) pointing tetrahedra as indicated by the labels u (d).

The gauge nature of the problem is simply a consequence of the local 3:1 constraint on each pyrochlore tetrahedron, or equivalently, that each diamond site is covered by a single dimer. To map this onto a more conventional gauge theory, we note further that the diamond lattice is bipartite, so we can define "up" (u) and "down" (d) sublattices corresponding to neighboring tetrahedra in the original pyrochlore lattice, as illustrated in Fig. 3. We can define thereby a discrete oriented electric field variable on the diamond lattice links, equal to zero if the corresponding pyrochlore site is a majority site, and equal to ±1 if the pyrochlore site is a minority one, choosing the field to always point from the up to the down diamond sublattice. We specify the spin-dimer configurations on the pyrochlore by a discrete variable $\hat{n}_i$ (i is a pyrochlore lattice site), such that

$$\hat{n}_i = \begin{cases} 0 & \text{majority site}, \\ 1 & \text{minority site}. \end{cases} \tag{2}$$

Mathematically, for the site i lying on the diamond link ab,

$$E_{ab} = \epsilon_a \hat{n}_{ab}, \tag{3}$$

where

$$\epsilon_a = \begin{cases} +1, & a \in u, \\ -1, & a \in d. \end{cases} \tag{4}$$

The electric field direction can be identified by the index ordering that gives it a positive value, as in Fig. 3.

The model we construct requires that each tetrahedron must include 1 minority site,

$$\hat{N}_a \equiv \sum_{i \in a} \hat{n}_i = 1, \tag{5}$$

where the label a identifies the various tetrahedra, and i is summed over pyrochlore lattice sites on tetrahedron a. See Fig. 3 for an illustration. This 3:1 constraint on the pyrochlore lattice in the QED formulation maps directly into

$$\epsilon_a = \mathrm{div}\, \vec{E}, \tag{6}$$

which is rather reminiscent of Gauss' law, where we have used the lattice divergence div $\vec{E}=\Sigma_b E_{ab}$. The "charge distribution" in this picture is that of alternating positive and negative charges on the diamond lattice. Positive charges sit on the u sublattice, and negative charges sit on the d sublattice.

A further consequence of this mapping is the presence of *global* topological charges, which are conserved in periodic (or infinite) systems. In particular, if one draws any surface not passing directly through diamond sites, the net electric flux through this surface is conserved. If this surface is compact and closed, this gives no additional information beyond the Gauss' law of Eq. (6). However, one may also consider noncompact surfaces that extend across the entire sample, and the electric flux through such surfaces is not determined by Gauss' law. A sufficient set of surfaces are the four nonparallel flat planes containing two-dimensional triangular lattices of pyrochlore sites (any two such parallel planes have the same electric flux). We denote the corresponding four electric fluxes by a four-vector (E_1,E_2,E_3,E_4). The fluxes may be chosen positive, and can in principle take any integer value from $0 \leqslant E_i \leqslant N_\Delta$, where N_Δ is the number of triangular sites in the plane. By the 3:1 (Gauss' law) constraint, the sum $E_1+E_2+E_3+E_4=N_\Delta$ is fixed. The electric flux sector containing the ground state varies with v.

It is conceptually useful to also map the full Hamiltonian of the model to a form more familiar in lattice QED. To do so, we must introduce the phase operator $\hat{\phi}_i$ conjugate to the number operator $\hat{n}_i$, satisfying

$$[\hat{\phi}_j,\hat{n}_i] = +i\delta_{ji}, \tag{7}$$

where δ_{ij} is the Kronecker delta function. The operator $e^{+i\phi_j}$ creates a minority site at site j, and using it we can construct any hopping term we wish for minority sites (down spins). With the canonical "rotor" variables $\hat{n}_i$, and $\hat{\phi}_i$, in principle an infinite set of number states with all integer eigenvalues of $\hat{n}_i$ are allowed. To faithfully represent the original spin-dimer model, therefore, we will include a large term U in the Hamiltonian which, in the limit $U\to\infty$, restricts the site occupancies to $\hat{n}_i=0,1$ as desired. We thereby obtain

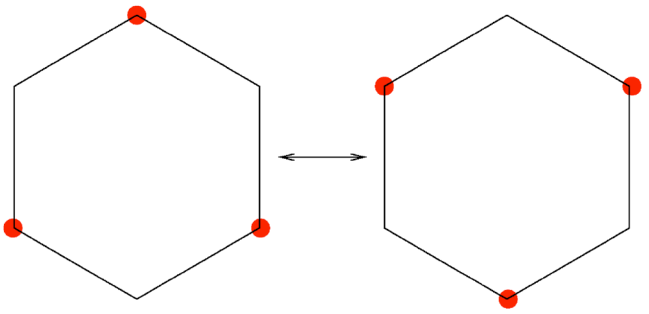

FIG. 4. (Color online) Ring exchange hopping on a hexagonal plaquette. The hopping flips between A and B type plaquettes, and is the only simple hopping event that preserve the one boson per tetrahedron constraint.

$$\begin{aligned}\mathcal{H} = &\frac{U}{2}\sum_i \hat{n}_i(\hat{n}_i-1) + U_t\sum_a (\hat{N}_a-1)^2 \\ &+ V\sum_{\hexagon} [\delta_{n_1,1}\delta_{n_2,0}\delta_{n_3,1}\delta_{n_4,0}\delta_{n_5,1}a_{n_6,0} + (n_i \leftrightarrow 1-n_i)] \\ &- \frac{K}{2}\sum_{\hexagon} (e^{+i(\phi_1-\phi_2+\phi_3-\phi_4+\phi_5-\phi_6)} + \mathrm{H.c.}).\end{aligned} \tag{8}$$

Here $\hexagon$ denotes the hexagonal plaquettes on the pyrochlore lattice, and the indices on ϕ enumerate the site (links) on the hexagon. The constraint operators $\hat{N}_a$ commute with $\mathcal{H}$ by construction, so for sufficiently large U_t the ground state will indeed satisfy Eq. (5). Moreover, when the constraint is enforced, the U_t term plays no further role. Formally, we are principally interested in the limit $U/K\to\infty$, as described above.

The K term when rewritten in this way appears as a rather complicated-looking multi-particle hopping amplitude. In fact, this form is actually the simplest one allowed by the constraint (5). The hopping of a down spin from one lattice site to another can be decomposed into a series of hops along nearest-neighbor links, so it is sufficient to analyze the simplest allowed moves. In general, the hopping on a nearest-neighbor link will violate (5) on two separate tetrahedra. Thus, any series of such hopping events will do the same. Analysis shows that it is only possible to hop between tetrahedra along closed contours. On the pyrochlore lattice the smallest closed contours are hexagonal plaquettes. Any other closed contour on the lattice can be constructed from these minimal moves, so we shall consider exclusively this "ring exchange hopping" on the hexagonal plaquettes. Such moves are illustrated in Fig. 4.

This Hamiltonian can now be reexpressed as a lattice gauge theory. Analogously to the definition of the electric field, we define the vector potential as

$$\mathcal{A}_{ab} = \epsilon_a \phi_{ab}. \tag{9}$$

The electromagnetic variables introduced above obey the same canonical commutation relations as $\hat{\phi}$ and $\hat{n}$, since $\epsilon_a^2=1$,

$$[\mathcal{A}_{ab}, E_{ab}] = i, \tag{10}$$

on the same link, and the commutator is 0 on different links. Note that from their definitions, E_{ab} is integer valued (and in particular $=0, \pm 1$) and A_{ab} is a 2π-periodic phase variable since the operator $e^{i\hat{\phi}}$ creates a particle.

In the new variables the ring exchange term becomes

$$e^{+i(\mathcal{A}_1+\mathcal{A}_2+\mathcal{A}_3+\mathcal{A}_4+\mathcal{A}_5+\mathcal{A}_6)} + \text{H.c.} = e^{+i\oint \vec{\mathcal{A}}\cdot d\vec{\ell}} + \text{H.c.} = 2\cos(\text{curl}\ \vec{\mathcal{A}})_{\hexagon}, \tag{11}$$

where we have introduced the lattice curl

$$(\text{curl}\ \vec{\mathcal{A}})_{\hexagon} = \sum_{\vec{r}\vec{r}' \in \hexagon} \vec{\mathcal{A}}_{\vec{r}\vec{r}'}. \tag{12}$$

In this form, the previously complicated-looking form of the K term becomes transparent.

After substituting the new variables, the Hamiltonian (8) takes the form

$$\mathcal{H} = \text{const} + \frac{U}{2}\sum_{\langle a,b\rangle}\left(E_{ab} - \frac{\epsilon_a}{2}\right)^2 - K\sum_{\hexagon}\cos(\text{curl}\ \vec{\mathcal{A}}) + V\sum_{\hexagon}(\delta_{\text{curl}\ \vec{E},3} + \delta_{\text{curl}\ \vec{E},-3}), \tag{13}$$

where the constant is a result of reorganizing the first term of (8) into a quadratic form. By identifying the curl of the vector potential with a magnetic field running through the plaquettes, $\vec{B} = \text{curl}\vec{\mathcal{A}}$,

$$\mathcal{H} = \text{const} + \frac{U}{2}\sum_{\langle a,b\rangle}\left(E_{ab} - \frac{\epsilon_a}{2}\right)^2 - K\sum_{\hexagon}\cos\vec{B} + V\sum_{\hexagon}(\delta_{\text{curl}\ \vec{E},3} + \delta_{\text{curl}\ \vec{E},-3}). \tag{14}$$

After these manipulations, the spin-dimer Hamiltonian has been formulated as a *compact* quantum electrodynamics in 3+1 dimensions. Equation (14) is very similar to the standard form of compact QED, but does differ from it by the presence of the rather ugly V term and the modification of the E^2 term by the $\epsilon_a/2$ "background field." Please recall also that we are expected to take the limit $U \to \infty$ to recover the spin and dimer model. Despite the differences, Eq. (14) does share all the same internal symmetries as the more conventional QED form. It is therefore expected to share the same properties in regimes where universality is mandated.

B. Phase diagram of the quantum spin and dimer model

Let us now return to the microscopic form of the spin-dimer model, and the question of the phase diagram. We will employ the QED formulation where useful in this analysis. For $v = V/K \to -\infty$, the off-diagonal K term can be neglected, and ground state is determined by minimizing the (negative) V term over *classical* spin/-dimer configurations. The solution is the R state, shown in Fig. 11. This state has only a discrete degeneracy, and is separated from other excited states by a gap [of $O(V)$], so it is expected to be stable to perturbation theory in K. Therefore the R state is the ground state for $v < v_{c1}$, with some $v_{c1} < 1$. In the R state, the electric flux is equally divided, $E_i/N_\Delta = 1/4$, apart from $O(1/N_\Delta)$ corrections for some frustrated boundary conditions.

For $v > 1$, the ground state can be found by rewriting the Hamiltonian as follows:

$$\mathcal{H}_{\text{QDM}} = K\sum_P (|\hexagon_A\rangle - |\hexagon_B\rangle)(\langle\hexagon_A| - \langle\hexagon_B|) + (v-1)K\sum_P (|\hexagon_A\rangle\langle\hexagon_A| + |\hexagon_B\rangle\langle\hexagon_B|). \tag{15}$$

In Eq. (15) $\mathcal{H}_{\text{QDM}}$ has been expressed as a sum of positive semidefinite projection operators, with coefficients that are all positive for $v > 1$. Therefore the energy is bounded below by zero, and any zero-energy state is a ground state. In particular, any classical state that contains no A or B hexagons is automatically a ground state. As a simple example, consider the "ferrimagnetic" state, with no enlargement of the unit cell but broken rotational symmetry. It is described as follows. On the diamond lattice, each vertex has four links emanating from it, which we label by $\mu = 0,1,2,3$. The ferrimagnetic state (oriented along a specific μ direction in space) has the same 3:1 arrangement on all identical tetrahedra. Explicitly, it can be written

$$|\text{Ferri}\rangle_\mu = \prod_{a \in u} |n_{a,\mu} = 1\rangle, \tag{16}$$

where the product is taken over the u sublattice of tetrahedra shown in Fig. 3. This state clearly obeys the 3:1 constraint (5)—one minority site on the μ corner of each tetrahedron. And moreover, it contains no A or B plaquettes, and hence is a zero-energy ground state for $v > 1$. The ferrimagnetic state is in the "furthest" topological sector from the R state, with $E_i = (N_\Delta, 0, 0, 0)$ (and permutations).

The ground states in this regime are, however, highly degenerate, and many other classical configurations are possible. All such states are "frozen" in that, for any value of v, they are exact eigenstates with trivial dynamics, being annihilated by the off-diagonal K term in Eq. (1).

At the point $v = 1$, Eq. (15) simplifies (the last term dropping out), but remains the sum of positive semidefinite projectors. This is the so-called Rokhsar-Kivelson (RK) point. The ground state space is enlarged, and contains now states in addition to the frozen ones. In particular, many configurations containing A and B hexagons are now allowed, provided the first projector in Eq. (15) annihilates the quantum state. One construction of this type is especially simple. Take a *uniform* superposition of *all* possible spin configurations, ignoring the 3:1 constraint. Now project this onto the 3:1 manifold. This is known as the RK wave function. It can be further broken into substates, e.g., by projecting out all the frozen states. It can also be projected into any of the electric flux sectors.

On reducing v to values slightly below unity, the second term in Eq. (15) becomes again nonzero but negative semidefinite. This indicates configurations with A and B hexagons are now preferred in the ground state. The frozen

states are then highly excited and energetically unfavorable. Instead, by an application of the reasoning of Ref. 6, the ground state can be argued to be a U(1) spin liquid state.

We summarize this argument, and the nature of the U(1) state. It is by now well known that RK wave functions for dimer models on bipartite lattices (like the diamond) display power-law equal-time correlations. These correlations may be understood as arising from the 3:1 constraint. In particular, the calculation of equal-time correlations in the RK state reduces to a problem of three-dimensional classical statistical mechanics: performing a statistical average over discrete electric field configurations subject to the Gauss' law constraint of Eq. (6). It turns out that the long-distance behavior of these correlations is captured simply by taking an effective classical free energy density proportional to $|\vec{E}|^2$ and treating $\vec{E}$ as a continuous Gaussian (but constrained) variable. The resulting correlations have a "dipolar" power-law form.[6,28]

By an argument originally due to Henley,[25] these power laws can be understood in the quantum theory as follows. Evidently, the discreteness of the electric field is unimportant at the RK point. Consequently, it is natural to treat $\vec{E}$ and $\vec{B}$ as continuous, write an effective action quadratic in these fields, and apply the Gauss' law constraint. However, there is an additional feature dictated by another peculiarity of the model. As we have pointed out already, all possible electric flux sectors are degenerate at the RK point. This implies that there should be no cost in the energy to shift $\vec{E}$ by a uniform constant (at the RK point). Henley's argument therefore indicates an appropriate effective Hamiltonian density is

$$\mathcal{H}_{\text{eff}} = a|\text{curl } \vec{E}|^2 + b|\vec{B}|^2 + \alpha(1-v)|\vec{E}|^2. \qquad (17)$$

The last $|E|^2$ term must vanish at the RK point, but is expected to become nonzero if one perturbs away from it. For $v=1$, this form can be shown to precisely reproduce the microscopically calculated correlations of the RK wave function, with specific constants a,b. For v larger than 1, the negative $|\vec{E}|^2$ term favors the sectors with "large electric flux," i.e., the frozen states, as expected, and $\vec{E}$ itself develops a nonzero expectation value. For v slightly less than 1, the positive $|\vec{E}|^2$ term instead favors the "minimal electric flux" sector with $E_i = N_\Delta/4$.

At low energies, for $v \lesssim 1$, therefore, it is expected that the a term above can be dropped in favor of the α term, making the effective Hamiltonian simply that of the usual non-compact QED. This indicates the system is in the "Coulomb phase" of the gauge theory, which has the usual properties expected of (3+1)-dimensional electrodynamics. In particular, unit test gauge charges can be introduced and interact via bounded $1/r$ Coulomb potentials. Such a gauge charge corresponds in the original pyrochlore magnet to a "spinon" excitation with fractional spin $\pm 3/2$. Thus the Coulomb phase is indeed a spin liquid, and in respect of the U(1) gauge structure, this state is called a U(1) spin liquid.

A key difference from standard "noncompact" QED *does* appear at nonzero energies, as a consequence of the fact that the $\vec{B}$ is defined modulo 2π. The divergence of this magnetic field is the sum of magnetic field values coming out of the plaquettes enclosing one cell in the diamond lattice. With the modulo 2π redundancy, configurations with div $\vec{B}$ an integer multiple of 2π are allowed. Thus, compact QED allows magnetic monopoles with quantized magnetic charge. These have a finite energy cost and are gapped excitations in the U(1) spin liquid.

Although the Coulomb phase emerges in a nontrivial way from the spin-dimer model in the vicinity of the RK point, we can mimic its low-energy physics more simply. In particular, the same phase is obtained from Eq. (14) by dropping the diagonal V term, and taking nonzero but finite U (instead of $U \to \infty$). This gives a "softened" model with the same universal properties as the original spin and dimer model. It is a remarkable fact that, by the preceding arguments, these two "sins" compensate each other and give the proper behavior of the original spin and dimer model for $v \lesssim 1$, in the Coulomb phase.

III. DUALITY AND MONOPOLE FORMULATION

On reducing v from values just below 1, eventually the spin-dimer model must undergo a transition out of the spin liquid state. The resulting state can be mimicked in the softened model by increasing U/K. The eventual outcome can be understood as follows. For $U \gg K$ the "magnetic field" term is subdominant, and so the electric field is a good quantum number. This limit is somewhat complicated in Eq. (14), because the U term selects two degenerate values $E_{ab}=0,\epsilon_a$ as low-energy states of each bond. Indeed this recovers the original effective spin-3/2 model, which is of course still non trivial. However, one can readily understand in this limit the basic nature of the other phases of the theory. To do so, we imagine generalizing the U term to include electric field interactions on nearby bonds. This will generally break the large U degeneracy in favor of some particular global arrangement of $E_{ab}=0,\epsilon_a$ values. Because of the discreteness of E_{ab}, deviations from this ground state are likewise discrete, any local rearrangement of the pattern results in a nonzero increase in energy, i.e., there is an energy gap. Gauge-neutral excitations are created in this way. Either a set of E_{ab} fields are modified along links forming a closed curve, or a pair of diamond lattice sites (on which the Gauss' law constraint is violated) is created, with a modified path of E_{ab} fields connecting them. The latter corresponds to a particle-antiparticle pair, and costs an energy proportional to the length of the path. Hence the pair itself is bound, the bound state being gauge neutral. The individual gauge-charged excitations are said to be confined by the linear potential between them. The confined phase corresponds to having the $\hat{n}_i$ operators certain in (8)—a Mott insulating phase, with some sort of diagonal ordering. In contrast to the Coulomb phase, the $\vec{B}$ field in the confining phase is very strongly fluctuating, so monopoles are no longer good excitations. In fact, it is appropriate to think of the confined phase as a Coulomb phase which has been destroyed by Bose condensation of monopoles. The presence of a delocalized monopole condensate can be thought of as leading to strong (gauge) magnetic fluctuations in the ground state.

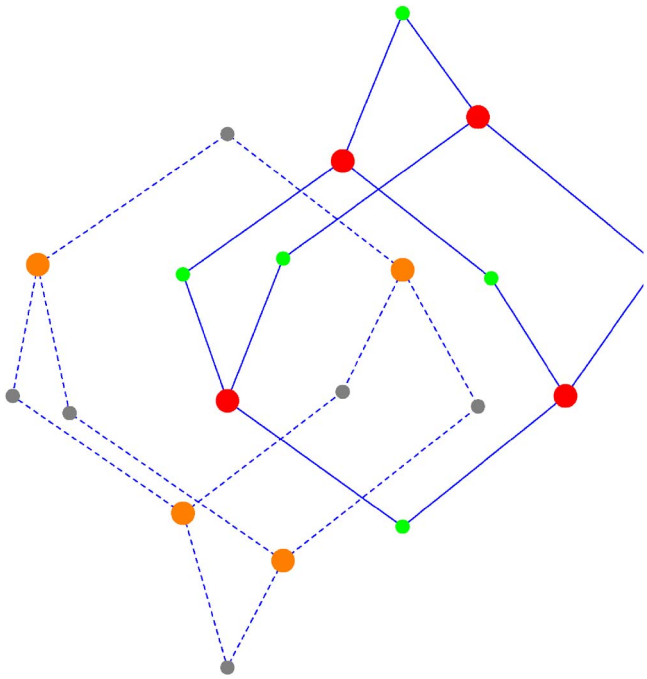

FIG. 5. (Color online) Direct and dual diamond lattices are dual to one another. The plaquettes of one lattice correspond to the links of its dual lattice.

We therefore wish to reformulate the lattice QED model so that the monopole excitations of the Coulomb phase are explicit. Here we follow Hermele *et al.*[6] with slight differences. As the reader will recall, the electric and magnetic fields in Maxwell's equations are dual when there are no charges or currents present. While there are no currents in our system, Eq. (6) shows we do have a charge distribution. The duality transformation is

$$\vec{E}_{ab} = \text{curl}\ \vec{\alpha} + \vec{e}^{(0)}_{ab}, \tag{18}$$

$$\vec{B} = \text{curl}\ \vec{\mathcal{A}}. \tag{19}$$

We have thus introduced an explicit operator for the magnetic field $\vec{B}$ and an "electric vector potential" $\vec{\alpha}$, whose exponential creates a 'magnetic field' since an exponential of $\vec{\mathcal{A}}$ creates an "electric field," via Eqs. (9), (4), (3), and (10). Here $\vec{e}^{(0)}$ is a classical electric field created by the charge distribution,[6] and

$$\text{div}\ \vec{e}^{(0)} = \text{div}\ \vec{E} = \epsilon_a. \tag{20}$$

It is convenient to choose $\vec{e}^{(0)}_{ab}$ to be integer valued, so that curl$\vec{\alpha}$ may also be taken integer valued. A simple choice is to take the classical configuration corresponding to one of the 3:1 states, e.g. just $e^{(0)}_{a,a+\mu} = \epsilon_a \delta_{\mu 0}$ (Fig. 5).

The Hamiltonian in the dual language takes the form

$$\mathcal{H} = \frac{U}{2}\sum_{\hexagon}\left(\text{curl}\ \vec{\alpha} + e^{(0)} - \frac{\epsilon_a}{2}\right)^2 - K\sum_{r,r'}\cos\vec{B}, \tag{21}$$

where we denote the sites of the dual lattice by r, and its links by r,r'. The hexagons now denote the plaquettes of the dual lattice. (Note the change in the summation subscripts on both the first and second terms.)

The dual fields obey the canonical commutation relations

$$[B_{r,r'}, \alpha_{r,r'}] = +i, \tag{22}$$

and the commutator vanishes for different links. The new fields are once again conjugate variables. $B_{r,r'}$ is defined modulo 2π—an angular variable, and the $\alpha_{r,r'}$ variable is integer valued.

Standard manipulations can now be used to "soften" the inconvenient integer constraint on $\alpha_{r,r'}$, remove the periodicity of $B_{r,r'}$, and make the monopole variables explicit. The reader is referred to Refs. 11 and 29 and references therein for details. These manipulations are inexact, but do not change the structure of the phase diagram in the vicinity of the transition from the Coulomb to confining phase. One obtains

$$\mathcal{H} = \frac{U}{2}\sum_{\hexagon}(\text{curl}\ \vec{\alpha} - \bar{e})^2 + \frac{K}{2}\sum_{r,r'}\vec{B}^2 - w\sum_{r,r'}\cos(\theta_r - \theta_{r'} - 2\pi\alpha_{r,r'}), \tag{23}$$

where now $\alpha_{r,r'}$ and $\vec{B}$ are real variables. In Eq. (23), one may freely shift $\bar{e}$ by a gradient, changing only the overall zero of energy, since such a gradient does not couple to curl$\vec{\alpha}$. We have used this freedom to modify the original $e^{(0)} + \epsilon_a/2$ terms to

$$\bar{e}_{a,a+\mu} = \epsilon_a\left(\frac{1}{4} - \delta_{\mu 0}\right), \tag{24}$$

which has no divergence, but has the same curl as the original "source" fields. As promised, explicit monopole degrees of freedom have been introduced. A monopole number operator N_r is slaved (by a dual Gauss' law constraint) to the $\vec{B}$ field,

$$\text{div}\ \vec{B} = 2\pi N_r. \tag{25}$$

It is conjugate to the dual phase θ_r, such that

$$[\theta_r, N_{r'}] = +i\delta_{r,r'}. \tag{26}$$

Equation (25) is another U(1) gauge constraint, so it is not surprising that the monopole hopping term w respects a dual (noncompact) gauge symmetry.

Although the monopole number N_r (which can be both positive or negative reflecting the two signs of flux emanating from a monopole) appears nowhere explicitly in Eq. (23), it is implicit through the constraint of Eq. (25). In the Coulomb phase for large K, therefore, monopoles are energetically costly (though their energy is finite, as is easily verified by integrating the associated B^2 energy density), with a gap of $O(K)$. Through the w term, however, monopoles do not reside in localized states with $N_r = \pm 1$, but instead in superpositions of such states, with only $\Sigma_r N_r = \pm 1$. As K is decreased, the monopole energy gap decreases, and at some point it will reach zero. This point corresponds to the confinement transition discussed in the previous section.

IV. FORMALISM—MONOPOLE DEFECTS ON THE DIAMOND LATTICE

A. Ground state manifold

To understand the confinement transition, we must understand the nature of the lowest energy monopole and antimonopole states, which condense at the transition. They are equivalent by $\vec{B} \to -\vec{B}$ symmetry, so it is sufficient to study just the monopole states. The ultimate field theory will consist of a relativistic field for each member of the monopole multiplet, since the relativistic description includes particles and antiparticles (here antimonopoles) on equal footing. We will apply for the most part a (dual) mean-field approach, taking curl $\alpha = \bar{e}$ in (23), and neglecting fluctuations of α around this value. This is sufficient to analyze the spectrum of ordered phases near the U(1) quantum liquid. Fluctuations will be restored later in Sec. VII.

We may thus consider the manifold of states with one monopole, i.e., $N_r = 1$ on one and only one site of the dual lattice, and $N_r = 0$ on all other sites. Through the w term in (23), the wave function of the monopole delocalizes, and is described by a tight-binding model, which we may write as

$$\mathcal{H}_{tb} = -w \sum_{\langle r,r' \rangle} [\psi^\dagger(r')\psi(r)e^{-i\alpha_{r,r'}} + \text{H.c.}], \tag{27}$$

where $\langle r, r' \rangle$ denotes a summation over nearest neighbors on the diamond lattice. Here $\psi_r^\dagger$ and ψ_r are creation and annihilation operators for the monopole. Note we have absorbed a factor of 2π into the vector potential relative to (23) to make our notation more conventional. By our mean-field assumption, $\alpha_{r,r'}$ is a c-number vector potential carrying a "flux" (actually electric flux) given by $2\pi\bar{e}$. Since it appears only in a periodic exponential, the form in Eq. (24) is equivalent to a flux of $2\pi/4 = \pi/2$ through each dual plaquette.

This can be understood as follows. The original compact QED theory had a staggered background charge of ϵ_a on each direct lattice site. The monopoles, as magnetic charges, see this in the same way electric charges would see a staggered lattice of magnetic monopoles and antimonopoles. These 'monopoles' and 'antimonopoles' (we use single quotes to denote the dual view, since these are actually the background gauge charges) are distributed in an alternating fashion at the center of each cell of the dual diamond lattice. The neighboring cells to a cell containing a 'monopole' all contain 'antimonopoles.' Each 'monopole' has a "charge" of 2π. Since all lattice directions are equivalent, the 'magnetic' flux going out of each face of the cell must be the same, as illustrated in Fig. 6. The structure of the diamond lattice is made of cells where each cell has 4 faces, as opposed to the cubic lattice which has six faces for each of its cells (cubes). Thus we conclude that each face in the diamond lattice has a flux of $2\pi/4 = \pi/2$ going through it in the direction from a 'monopole' cell to an 'antimonopole' cell. The ψ_r monopole particle thus experiences Aharonov-Bohm fluxes of precisely this sort as it moves through the lattice.

It proves convenient to describe the links of the diamond lattice by $(r, r') = (a, \mu)$ where $a \in u$ denote the sites of the u sublattice, and $\mu \in \{0,1,2,3\}$ enumerate the four links emanating from each u site. Furthermore, we can enumerate the u sublattice sites by $\vec{r} = \Sigma_{j=1}^{3} n_j \vec{a}_j$ where $\vec{a}_j$ $[\vec{a}_1 = (a/2)(\hat{y} + \hat{z}), \vec{a}_2 = (a/2)(\hat{x} + \hat{z}), \vec{a}_3 = (a/2)(\hat{x} + \hat{y})]$ are the primitive Bravais lattice vectors of the fcc lattice, and n_j span the integer numbers. We refer to this coordinate system as "index" space.

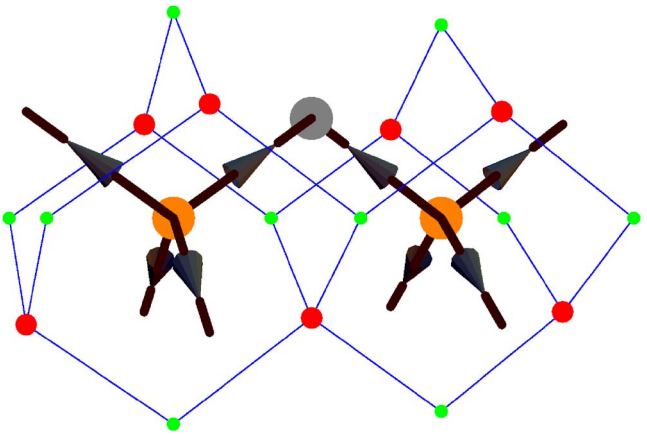

FIG. 6. (Color online) Alternating charge distribution emits 'magnetic' field lines through the faces of a diamond lattice cell.

We shall now focus our attention on finding the ground state manifold of this Hamiltonian. First we must find an appropriate choice of the vector potential giving the desired flux pattern through the faces inside the lattice. To this end, the index space notation proves particularly useful. One such possible vector potential is

$$\alpha_0(\vec{n}) = 0, \quad \vec{\alpha}(\vec{n}) = (\alpha_1(\vec{n}), \alpha_2(\vec{n}), \alpha_3(\vec{n})) \equiv \vec{\epsilon}(\vec{Q} \cdot \vec{n}), \tag{28}$$

where $\vec{Q} = (\pi/2)(1, 0, -1)$ and $\vec{\epsilon} = (1, 1, 2)$ (Fig. 7).

We proceed to diagonalize the hopping term. General eigenstates cannot be found analytically, however minimum energy eigenstates can. We find eight ground state eigenmodes, denoted Φ_ν and $\bar{\Phi}_\nu$ where the indices run through

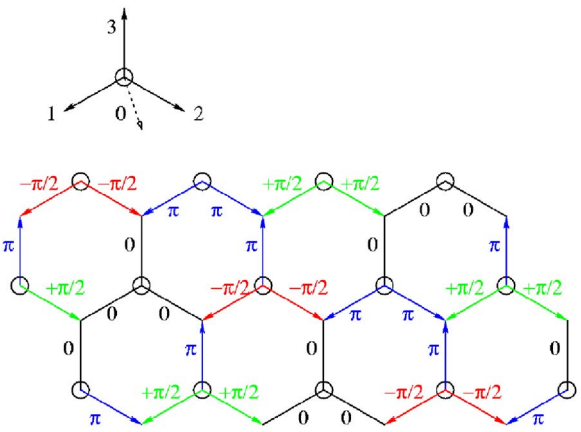

FIG. 7. (Color online) Projected diamond plane view of vector potential pattern—links between the honeycomb planes have $\alpha_0 = 0$. All links with the same vector potential value are in the same color.

$\nu=0,1,2,3$. The details of the eight eigen-modes are are left for Appendix A.

B. Symmetries

The eight k-space minima can be related by the symmetries of the Hamiltonian. Each one of the symmetries is represented by an operator that commutes with the Hamiltonian. However, some of the symmetry operators do not commute with each other. If we choose to represent the Hilbert subspace of the minimum energy states of the Hamiltonian using a basis of eigenstates that are also eigenstates of a symmetry operator $\hat{S}_1$, then for a different operator $\hat{S}_2$ with which it does not commute $[\hat{S}_1,\hat{S}_2]\neq 0$ the basis states will not be eigenstates of $\hat{S}_2$. Thus by acting with $\hat{S}_2$ on the eigenstates of $\hat{S}_1$, one may generate another linearly independent eigenstate of the Hamiltonian with the same energy. Such a structure therefore constrains the minimum size of ground state multiplets. This idea should be familiar from the representation theory of SU(2) in standard quantum mechanics.

While the symmetry group of the diamond lattice is the space group $Fd\bar{3}m$,[30] the dual Hamiltonian itself transforms under a *projective symmetry group* (PSG), since a vector potential α appears explicitly. The PSG differs from the space symmetry group by a specific gauge transformation accompanying every space symmetry operation.

We can describe the entire symmetry group using a reduced set of operators—generators—from which any symmetry operation can be constructed as a product of members in the reduced set. One can find a minimal such reduced set. We shall consider the minimal set of the point symmetry group, as well as the three primitive translations. We leave the complete description of the PSG to Appendix B, and only state here that the reduced set comprises three (fcc) translations t_j, a reflection symmetry i, an inversion symmetry p, a twofold rotation symmetry r_2, and a threefold rotation symmetry r_3.

Our convention is to denote symmetry operations in the space symmetry group by lowercase letters, and the corresponding PSG operations by uppercase letters. The space group obeys some group algebra, which is just a multiplication table. It can be constructed by imposing a set of algebraic rules on the generators alone, of the form

$$\hat{s}_1\cdots\hat{s}_n=1, \tag{29}$$

where $\hat{s}_i$ are generators. The details of these relations are left to Appendix C.

To obtain the PSG we must add gauge transformations to each of these symmetry operations. Consider a symmetry operation $\hat{S}$ with the following action on the lattice sites in real space coordinates $\hat{s}:r\rightarrow r'$. Now add a gauge transformation to accompany the lattice site transformation

$$\hat{S}:\psi(r)\rightarrow\psi(r')e^{-i\Lambda(r)}. \tag{30}$$

Let us examine what this transformation does to a generic hopping term in the Hamiltonian

$$\hat{S}:\psi^{\dagger}(r_2)\psi(r_1)e^{-i\alpha_{r_1,r_2}}\rightarrow\psi^{\dagger}(r_2')\psi(r_1')e^{+i[\Lambda(r_2)-\Lambda(r_1)-\alpha_{r_1,r_2}]}. \tag{31}$$

We require that the Hamiltonian be invariant under this transformation, and so we must have

$$e^{+i[\Lambda(r_2)-\Lambda(r_1)-\alpha_{r_1,r_2}]}=e^{-i\alpha_{r_1',r_2'}}, \tag{32}$$

or put more simply

$$\Lambda(r_2)-\Lambda(r_1)-\alpha_{r_1,r_2}=-\alpha_{r_1',r_2'}\pmod{2\pi}. \tag{33}$$

Using this procedure we can find the appropriate gauge transformations for each of the symmetry operations in our reduced set. We leave the details to Appendix B.

The PSG has a modified group algebra. The relations among the generators differ only slightly from those in the space group, which are given in Eq. (C1). Consider any succession of symmetry operations that takes every site on the lattice back to itself. The same succession of the "gauged" operations can therefore only perform a gauge transformation on the lattice model. Since all the gauged symmetry operations leave the Hamiltonian invariant, and the various terms in the Hamiltonian depend explicitly on the vector potential, any gauge transformation that is not uniform (a global gauge transformation) will modify the vector potential by introducing nonzero gradients in the gauge transformation. We conclude, therefore, that any succession of symmetry operations that leave the lattice sites in place can only undergo an additional global gauge transformation when those operations are gauged. A rule in the algebra (29) is in general modified into

$$\hat{S}_1\cdots\hat{S}_n=e^{+i\theta}, \tag{34}$$

where θ is some angle. The PSG algebra differs from the space symmetry group algebra (C1) only in the following rules:

$$t_{j+1}\cdot t_j\cdot {t_{j+1}}^{-1}\cdot {t_j}^{-1}=1 \tag{35}$$

in the space algebra, and

$$\hat{T}_{j+1}\cdot\hat{T}_j\cdot{\hat{T}_{j+1}}^{-1}\cdot{\hat{T}_j}^{-1}=-i \tag{36}$$

in the PSG algebra.

The eight ground state modes we found span the ground state manifold, and so any linear combination of these states is also a ground state,

$$\Psi=\sum_{\nu=0}^{3}(\phi_{\nu,u}\Phi_{\nu}+\phi_{\nu,d}\bar{\Phi}_{\nu}), \tag{37}$$

where $\phi_{\nu,a}$ now denote the complex amplitudes of the eight eigenmodes. Given the symmetry operations in momentum space, we find the ground state manifold is closed and completely connected—no disconnected subsets of the manifold exist.

We now assume that these eight fields are slowly varying with position on the lattice, so we can treat them using a continuum limit. However, these eight fields will still be required to respect the symmetry of the underlying lattice.

The eight slowly varying fields $\phi_{\nu,a}$ transform under a particular eight-dimensional irreducible representation (irrep) of the PSG. In fact, we prove in Appendix F that this is the minimum dimension of a representation of the PSG. It is convenient to change the field basis to

$$\phi_{0u} = \frac{\zeta_0 + \zeta_1}{\sqrt{2}}, \quad \phi_{2u} = \frac{\zeta_0 - \zeta_1}{\sqrt{2}},$$

$$\phi_{1u} = \frac{\zeta_2 + \zeta_3}{\sqrt{2}}, \quad \phi_{3u} = \frac{\zeta_2 - \zeta_3}{\sqrt{2}},$$

$$\phi_{0d} = \frac{\xi_0 + \xi_1}{\sqrt{2}}, \quad \phi_{2d} = \frac{\xi_0 - \xi_1}{\sqrt{2}},$$

$$\phi_{1d} = \frac{\xi_2 + \xi_3}{\sqrt{2}}, \quad \phi_{3d} = \frac{\xi_2 - \xi_3}{\sqrt{2}}. \tag{38}$$

This basis realizes a "permutative representation" of the PSG, in the nomenclature of Ref. 1. That is, the symmetry operations of the PSG act on these fields by a combination of permutations and simple diagonal phase rotations. See Eqs. (D1)–(D6). Because of this structure, the action takes a particularly simple form in this basis.

C. Effective low-energy action

Our goal is to describe a low-temperature condensate phase of the monopole defects. Limiting the discussion to zero temperature, we set out to construct a phenomenological Landau-Ginzburg (LG) action to access the condensate phase. We concentrate on the ground state manifold of the monopole defects, ignoring any higher energy modes, and construct a low-energy effective continuum action in the eight field components of (37). The various terms allowed in the action must be invariant under the PSG in the eight-dimensional representation (D1)–(D6). As the effective action will live in a (3+1)-dimensional spacetime, we seek terms only up to quartic order in the field operators—any higher-order terms will be irrelevant in the renormalization group sense.

To quadratic order only one invariant exists,

$$\Theta_1 = \sum_j (|\zeta_j|^2 + |\xi_j|^2), \tag{39}$$

a typical mass term, where the indices enumerate $j = 0,1,2,3$.

At quartic order we find four invariants

$$(\Theta_1)^2 = (|\vec{\zeta}|^2 + |\vec{\xi}|^2)^2,$$

$$\Theta_2 = \sum_{i \neq j} |\zeta_j|^2 |\zeta_i|^2 + \sum_{i \neq j} |\xi_j|^2 |\xi_i|^2,$$

$$\Theta_3 = |\vec{\zeta}|^2 |\vec{\xi}|^2, \quad \Theta_4 = \sum_{ijkl} \kappa_{ij}^{kl} \zeta_k \xi_l \zeta_i^* \xi_j^*, \tag{40}$$

where the sums over indices are always over 0, 1, 2, 3 unless otherwise stated, and the vector notation implies a four-component vector. We shall not specify the κ tensor explicitly, as it is long and complicated. We leave it to Appendix E.

The new set of independent terms obeys numerous continuous symmetries in a rather transparent manner (for brevity we do not specify the discrete symmetries of these terms).

(1) Θ_1 is invariant under a full U(8) symmetry, as it is just the norm of an eight-dimensional complex coordinate vector.

(2) Θ_2 is invariant under a $[\mathrm{U}(1)]^8$ symmetry, since it depends only upon the magnitudes of the field components in the new basis. We may change freely and independently the phase of each field component.

(3) Θ_3 is invariant under a $\mathrm{U}(4) \times \mathrm{U}(4)$ symmetry, because it involves only the norm of two four-dimensional complex vectors.

(4) Θ_4 obeys a $[\mathrm{U}(1)]^2$ symmetry group corresponding to the following transformation:

$$\forall j \quad \zeta_j \to e^{+i\delta} \zeta_j, \quad \xi_j \to e^{+i\lambda} \xi_j. \tag{41}$$

The action as a whole is invariant under a $[\mathrm{U}(1)]^2$ symmetry, governed by the Θ_4 invariant.

The only microscopic symmetry of the action is the dual U(1) gauge invariance, i.e., identical phase rotations of all field components. This changes just the overall phase of the monopole wave function, and has no physical consequence (it is a true gauge). The other "staggered" U(1) rotation [with $\delta = -\lambda$ in Eq. (41)] is accidental, occurring only in the proximity of the critical point at which truncation to the quartic action is a good first approximation. It will be broken if we include sufficiently high-order terms in the action. Our investigation concluded that the staggered U(1) symmetry persists at 6th order, but ultimately breaks down to a discrete symmetry (Z_4) at eighth order. The remaining discrete symmetry Z_4 can be identified as part of the lattice PSG.

Finally, the most general low-energy effective action up to quartic order is

$$\mathcal{S} = \int_{\mathbf{r},\tau} \Big(|(\partial_\mu - i\alpha_\mu)\zeta_j|^2 + |(\partial_\mu - i\alpha_\mu)\xi_j|^2 + \tilde{\gamma}\Theta_1 + \gamma_1 \Theta_1^2 + \gamma_2 \Theta_2 + \gamma_3 \Theta_3 + \gamma_4 \Theta_4 + \frac{1}{2e^2} F^2 \Big), \tag{42}$$

where a sum over j, as well as integration over spacetime are implied, and $(1/2e^2)F^2$ is the Maxwell term in the action, with $F_{\mu\nu} = \partial_\mu \alpha_\nu - \partial_\nu \alpha_\mu$. Here α is the continuum version of the vector potential α appearing in Eq. (27). The γ_j are phenomenological couplings undetermined in our theory.

Higher-order terms can be ignored for a renormalization group (RG) analysis (in 3+1 dimensions, they are irrelevant in the RG sense, and can be treated perturbatively when necessary), but must be taken into account in a mean-field analysis to which we now turn.

V. MEAN-FIELD THEORY

We now turn to analyze our effective action (42). Using mean-field theory (MFT) we can find the various phases of this action. Replacing the fields with their average values, we

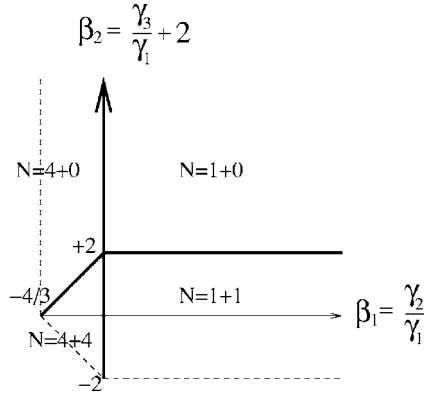

FIG. 8. Two-dimensional mean-field theory phase diagram (β_2 vs β_1) of simplified free energy, $\beta_3=0$. The phases exist only within the bounds of the dashed lines. The thick continuous lines show boundaries between the different phases.

obtain a Lagrangian density $\mathcal{L}$ that must be minimized with respect to the field averages.

At first we ignore the Θ_4 term, since it has the lowest symmetry. We shall examine only the ordered phases which occur for weak γ_4 (and higher-order coefficients γ_5, γ_6 when necessary—see below) for simplicity. Scaling all the couplings to that of ${\Theta_1}^2$ we get

$$M^2 = -\frac{\tilde{\gamma}}{\gamma_1}, \quad \beta_1 = \frac{\gamma_2}{\gamma_1}, \quad \beta_2 = \frac{\gamma_3}{\gamma_1} + 2, \quad \beta_3 = \frac{\gamma_4}{\gamma_1}. \tag{43}$$

The mean-field Lagrangian density with $\beta_3=\gamma_4=0$ is

$$\mathcal{L}/\gamma_1 = \left(-M^2|\vec{\zeta}|^2 + (|\vec{\zeta}|^2)^2 + \beta_1 \sum_{i\neq j} |\zeta_j|^2|\zeta_i|^2\right) + (\zeta \to \xi) + \beta_2 |\vec{\zeta}|^2|\vec{\xi}|^2. \tag{44}$$

We first find the mean-field minima with $M^2>0$ in the $\beta_{1,2}$ plane. The resulting phase diagram is illustrated in Fig. 8. We label the "phases" by the number of nonzero components of $\vec{\xi}$ and $\vec{\zeta}$, ordered from largest to smallest, with the notation N_1+N_2. The "phases" are as follows.

$\beta_1>0, \beta_2>2$. In this region, only one field component condenses, so this region is labeled 1+0.

$\beta_1>0, -2<\beta_2<2$. Here one field component of each set (ζ_i, ξ_j) condenses, so this is a 1+1 region.

$\beta_1<0, \beta_2>2\left(1+\beta_1 \frac{3}{4}\right)$. Here all the field components of one of the two sets condense, denoted 4+0.

$\beta_1<0, -2\left(1+\beta_1 \frac{3}{4}\right)<\beta_2<2\left(1+\beta_1 \frac{3}{4}\right)$. Here all the eight field components are nonzero, so it is a 4+4 region.

It should be pointed out that specifying the number of nonzero components of the *complex* fields does not necessarily specify a unique charge-ordered *phase* of the problem. Physically, these charge-ordered states break only discrete space group symmetries, and so are expected to lead to only a discrete degeneracy of ground states. In our dual gauge formulation, each physically distinct state is represented by a "cycle" in the monopole field space, along which the phase of all the fields is varied together by a uniform angle which can go from 0 to 2π. This variation has no physical significance since this is a gauge symmetry. Other continuous phase freedoms of the mean field solutions, which do not vary the phases of all components identically, are however not a pure gauge freedom. Such a (artificial) freedom can only be a result of truncating the dual action to quartic order.

In fact, only the 1+0 phase lacks any such "emergent" phase freedom. In particular, the different 1+0 states obtained by choosing each of the eight possible components nonzero are physically distinct, and the phase of this nonvanishing field is pure gauge, with no physical significance. Thus, the 1+0 states are eightfold degenerate. The β_3 term vanishes for such states and does not change this conclusion. These states exhibit an enlarged unit cell, comprising four unit cells of the underlying lattice, and containing 16 pyrochlore lattice sites. (In fact, we will find that all our mean-field states have an enlarged unit cell. The amount by which the unit cell is enlarged can be computed by explicitly checking how a given mean-field state transforms under an arbitary translation using the PSG.) The Bravais lattice formed by these enlarged unit cells is simple cubic (sc). It is noteworthy that this phase is the R state found in Ref. 13.

The other 1+1, 4+0, and 4+4 solutions retain at least some physically meaningful phase freedom even when β_3 is included in the action. Consider first the 4+0 case. For such configurations, the β_3 term vanishes, so the phases of all four nonzero fields remain free at quartic order. Only the overall phase of the four fields is gauge, and hence will remain undetermined—and unphysical—to all orders. To fix the remaining three phases, we must consider higher-order terms. In this case, sixth order is sufficient, and there is one term which resolves the continuous degeneracy:

$$\mathcal{L}_6 = \gamma_5 \,\mathrm{Re}\{e^{-i\pi/4}[(\zeta_0^*)^3\zeta_1\zeta_2\zeta_3 - (\zeta_1^*)^3\zeta_0\zeta_2\zeta_3 - (\zeta_2^*)^3\zeta_0\zeta_1\zeta_3 + (\zeta_3^*)^3\zeta_0\zeta_1\zeta_2] - (\vec{\zeta}\to\vec{\xi})\}. \tag{45}$$

In the $N=4+0$ phase for $\gamma_5>0$, one minimum energy state is

$$\vec{\zeta} = (1, e^{+i3\pi/4}, e^{+i\pi/4}, 1). \tag{46}$$

It is part of a set of 792 total states, which can be generated from this one by the PSG. For $\gamma_5<0$, one configuration is

$$\vec{\zeta} = (1, e^{+i\pi/4}, e^{+i\pi/4}, 1), \tag{47}$$

which is part of a set of 384 degenerate states connected by the PSG. The enlarged unit cell comprises 16 unit cells of the original lattice, and contains 64 pyrochlore lattice sites. The "supercells" are arranged in a body-centered cubic (bcc) Bravais lattice.

In the 1+1 case, there is a single undetermined physical phase, an opposite phase rotation of $\vec{\zeta}$ and $\vec{\xi}$. This is a direct result of the "staggered" U(1) symmetry of the action at sixth order. Any such solution breaks this staggered U(1), and so making such a rotation gives a different solution. The staggered U(1) symmetry is broken only at eight order, by 8 distinct terms. In the 1+1 case, only one of these terms is nonvanishing. It takes the form

$$\mathcal{L}_8 = \gamma_6 \,\mathrm{Re}\{[(\zeta_0^*)^4 - (\zeta_1^*)^4 - (\zeta_2^*)^4 + (\zeta_3^*)^4] \times [\xi_0^4 - \xi_1^4 - \xi_2^4 + \xi_3^4]\}. \quad (48)$$

The nature of the phase depends upon the sign of γ_6. In each case, there are 64 physically distinct ground states: four choices each for the nonzero component of $\vec{\zeta}, \vec{\xi}$, and four inequivalent phase minima of Eq. (48).

Of the many states we mention one configuration for $\gamma_6 < 0$,

$$\zeta_0 = \xi_0 = 1, \quad (49)$$

and one configuration for $\gamma_6 > 0$,

$$\zeta_0 = e^{-i\pi/4}\xi_0 = 1. \quad (50)$$

The enlarged unit cell comprises 16 unit cells of the original lattice, and contains 64 pyrcohlore lattice sites. The "supercells" are arranged in a simple hexagonal Bravais lattice, with a ratio of $c/a = 4\sqrt{1.5}$ in standard notation.

In the 4+4 case the relative phases in each quartet are determined at fourth order by β_3, and the same "staggered" U(1) symmetry as in the 1+1 case remains.

For $\gamma_4 > 0$ one possible configuration is

$$\vec{\zeta} = (1, e^{+i\pi/4}, e^{+i\pi/12}, e^{-i\pi/6}),$$

$$\vec{\xi} = e^{+i\lambda_4}(1, e^{+i7\pi/12}, e^{+i7\pi/12}, e^{-i\pi/2}), \quad (51)$$

and for $\gamma_4 < 0$ a possible configuration is

$$\vec{\zeta} = (1, e^{+i\pi/4}, e^{+i3\pi/4}, e^{+i\pi/2}),$$

$$\vec{\xi} = e^{+i\lambda_4}(1, e^{-i3\pi/4}, e^{-i3\pi/4}, e^{-i\pi/2}). \quad (52)$$

Many (over 10 000 in each case) other configurations are possible, and connected via the PSG to this state.

The "staggered" U(1) symmetry is lifted by various eighth-order terms. Depending on the various couplings of the eighth-order terms, we get that the staggered U(1) breaks into the same two Z_4 multiplets as the 1+1 state does. We shall not belabor the details of all eight of these terms. Equation (48) alone suffices to access both multiplets. For $\gamma_6 > 0$

$$\lambda_4 - \lambda_0 = \frac{\pi}{4} + n\frac{\pi}{2} \quad (53)$$

and for $\gamma_6 < 0$

$$\lambda_4 - \lambda_0 = n\frac{\pi}{2}. \quad (54)$$

Finally, in any one of these cases, the enlarged unit cell comprises $4 \times 4 \times 4 = 64$ unit cells of the original lattice, and therefore contains 256 pyrochlore lattice sites. The "supercells" are arranged in a face-centered cubic Bravais lattice, with the primitive lattice vectors taken four times larger relative to the original fcc lattice.

Using a direct mapping between the monopole defect density and the spin density variations described in the next section, we can depict the latter in Figs. 9–19

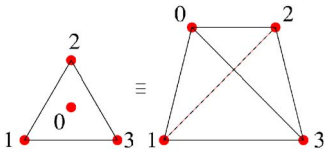

FIG. 9. (Color online) Notation for the spin density pictures. Triangles with a site at the center represent up-pointing tetrahedra. Triangles with no site at the center represent down-pointing tetrahedra.

VI. ORDERING PATTERNS

Having found the various allowed monopole defect condensate phases in the abstract order parameter space by algebraic considerations, we want to identify the physical spin (S_i^z) ordering patterns in each case.

The density of the monopole defects is a varying scalar density. As it is the only spatially varying scalar in the problem, the spin density must have similar spatial variation. More precisely, both densities must obey the same symmetries,

$$\rho(\vec{r}_i) \sim \langle S_i^z \rangle, \quad (55)$$

where $\rho(\vec{r})$ is the monopole defect density. The monopole defect density can be found by taking the wave function (37) squared,

$$\rho(\vec{r}) = |\Psi(\vec{r})|^2. \quad (56)$$

The resulting density is now a function of the field values $\phi_{\nu,a}$. By inserting the values for the different MFT phases, we can recover the density.

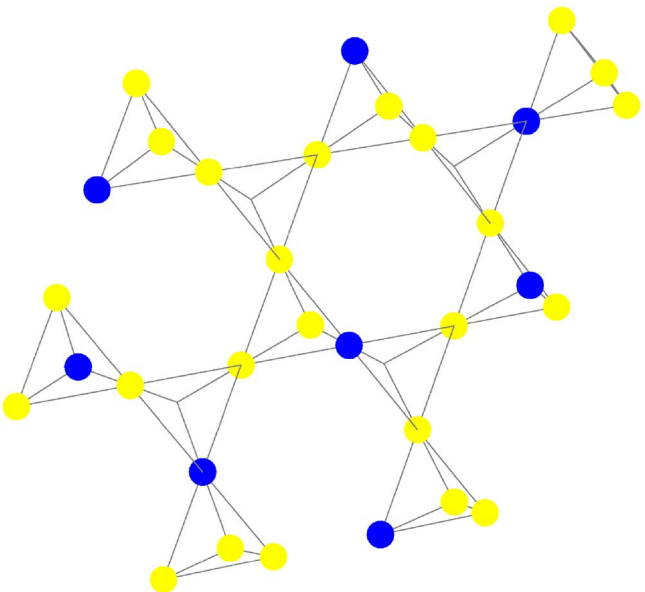

FIG. 10. (Color online) The spin density variations in the 1+0 phase—a three-dimensional image. One field component only has a nonvanishing expectation value. Here only minority sites in one Kagome plane and in the triangular plane "above" the page are shown. Those in the triangular plane "below" the page are omitted to keep the image uncluttered.

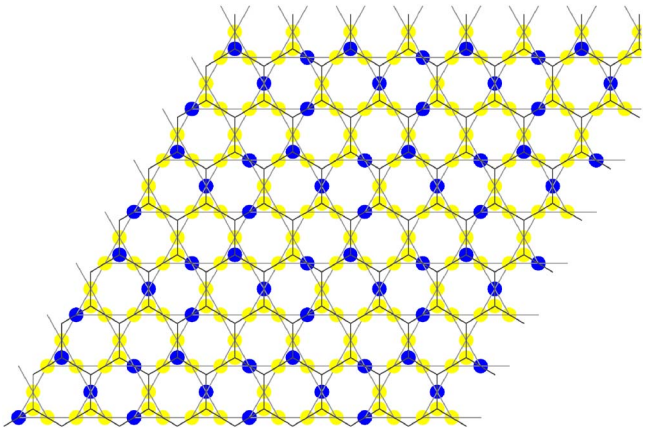

FIG. 11. (Color online) The spin density variations in the 1+0 phase—same phase as in Fig. 10 for comparison. This phase has an enlarged unit cell of $2\times2\times1=4$, in a simple cubic Bravais lattice.

In some phases, however, the symmetry breaking is not manifest in the scalar density, but rather in the current or kinetic energy:

$$J_{r,r'} = i[\Psi^*(\vec{r}')\Psi(\vec{r})e^{-i\alpha_{r,r'}} - \text{c.c.}],$$

$$K_{r,r'} = [\Psi^*(\vec{r}')\Psi(\vec{r})e^{-i\alpha_{r,r'}} + \text{c.c.}]. \tag{57}$$

Both the current density and the local kinetic energy can be encoded in a complex valued vector,

$$v_{r,r'} = \Psi^*(\vec{r}')\Psi(\vec{r})e^{-i\alpha_{r,r'}}. \tag{58}$$

The imaginary and real parts will give us (half) the current density and the local kinetic energy, respectively.

Each plaquette in the dual diamond lattice corresponds to a pyrochlore lattice site at the center of the plaquette. Any monopole defect "object" we can define on the dual plaquettes is also defined on the direct pyrochlore lattice sites, and encodes the symmetry of the MFT phase. Therefore, the function must be "similar" to the spin density on these sites, in the sense of giving the correct symmetry of the latter. An appropriate function is a loop integral (curl) of the complex current around the plaquette

$$\sum_{\vec{r}\vec{r}' \in \hexagon} v_{\vec{r}\vec{r}'} \sim n_{\hexagon} = n_i. \tag{59}$$

We can formalize this argument by considering Maxwell's equations, with magnetic monopoles

$$\text{curl}\ \vec{E} = -\frac{\partial \vec{B}}{\partial t} + \vec{J}_b, \quad \text{curl}\ \vec{B} = +\frac{\partial \vec{E}}{\partial t} + \vec{J}_e,$$

$$\text{div}\ \vec{E} = \rho_e, \quad \text{div}\ \vec{B} = \rho_b, \tag{60}$$

where the magnetic monopole density and current are denoted with a subscript b. In a static system integrating the first equation over some surface we get, by Stokes theorem,

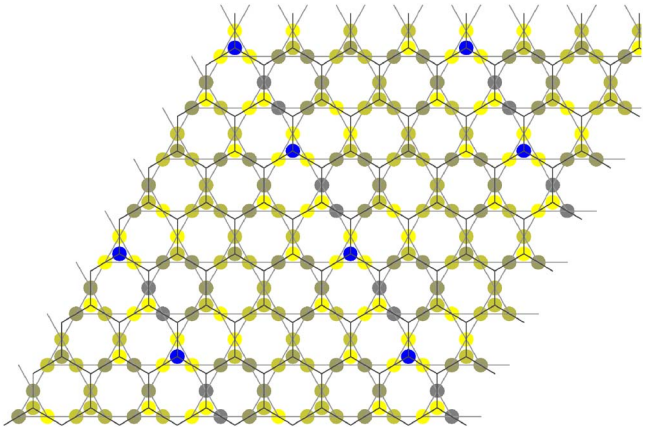

FIG. 12. (Color online) The spin density variations in the 1+1 phase, for $\gamma_5<0$. One each of the four ζ and ξ fields has a nonvanishing expectation value. The expectation values have identical magnitude. This phase has an enlarged unit cell of $2\times4\times2=16$, in a simple hexagonal Bravais lattice.

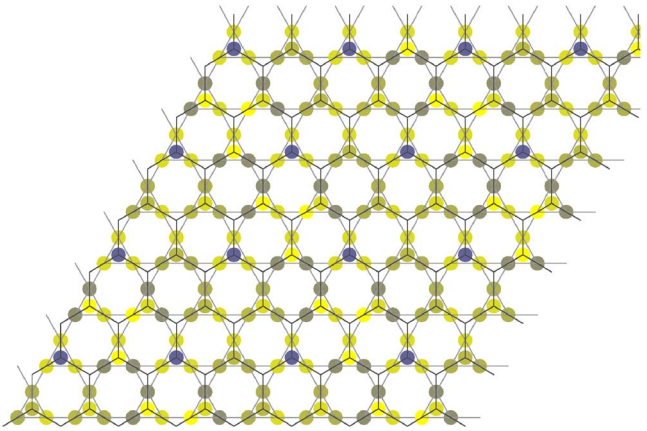

FIG. 13. (Color online) The spin density variations in the 1+1 phase, for $\gamma_5>0$. One each of the four ζ and ξ fields has a nonvanishing expectation value. The expectation values have identical magnitude. This phase has an enlarged unit cell of $2\times4\times2=16$, in a simple hexagonal Bravais lattice.

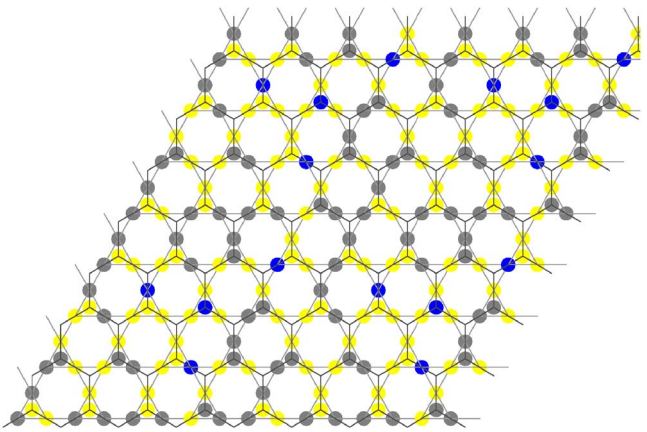

FIG. 14. (Color online) The spin density variations in the 4+0 phase, for $\gamma_4>0$. The four field components of either the ζ or ξ set have a nonvanishing expectation value of identical magnitude. This phase has an enlarged unit cell of 16, in a bcc Bravais lattice.

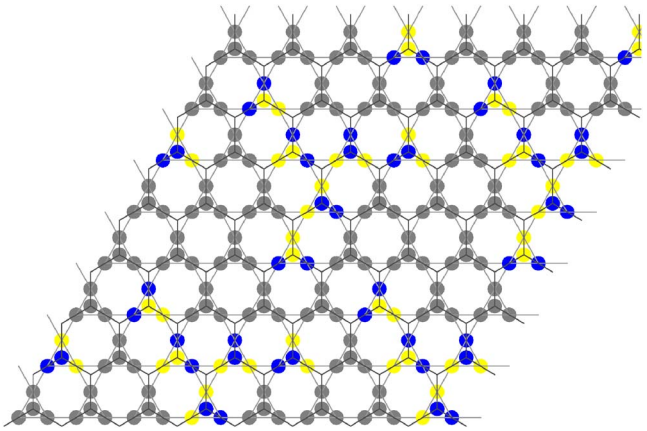

FIG. 15. (Color online) The spin density variations in the 4+0 phase, for $\gamma_4 > 0$. The four field components of either the ζ or ξ set have a nonvanishing expectation value of identical magnitude. This phase has an enlarged unit cell of 16, in a bcc Bravais lattice.

$$\oint_C \vec{J}_b \cdot d\vec{\ell} = \oint_C \text{curl}\, \vec{E} \cdot d\vec{\ell} = \int_S \vec{E} \cdot d\vec{A}. \tag{61}$$

From this last expression it is evident that the loop integral of the monopole defect current gives the electric flux through that loop. The lattice version of the electric flux is a constant plaquette "area" times the electric field penetrating perpendicular to that plaquette

$$\sum_{\vec{r}\vec{r}' \in \hexagon} J_{\vec{r}\vec{r}'} = E_{ab} \sim n_i. \tag{62}$$

In conclusion the variations in the spin density can be related to the loop sums of the monopole defect current around plaquettes of the dual diamond lattice. Armed with this knowledge we can plot a function to show the spin density variations. We plot the "spin density" so defined for each of the phases obtained in mean field theory in Figs. 11–19.

VII. RG ANALYSIS

In this section, we briefly consider the effect of fluctuations on the mean-field critical behavior of our effective action. Our primary focus in this paper is not on quantum critical phenomena, but rather on the nature of the ordered phases *close* to the U(1) spin liquid state. These results for the ordered phases are independent of the contents of this section.

By simple power counting, the problem of a generalized "Ginzburg-Landau" theory in 3+1 dimensions (with a many-component "superconducting" field φ_ℓ) is in its upper critical dimension, so one expects either of two possibilities. One possibility is that the Gaussian fixed point is marginally stable, and mean-field behavior is correct up to logarithmic factors. The other possibility is that the Gaussian fixed point is marginally unstable, and the true critical behavior is a strong coupling problem; most probably, such flows to strong coupling indicate a weak fluctuation-induced first-order transition.

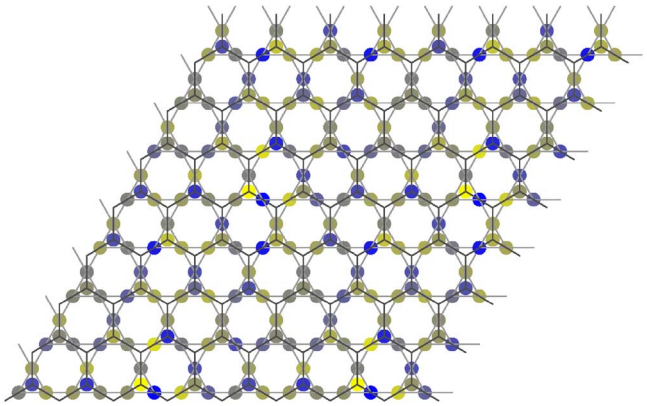

FIG. 16. (Color online) The spin density variations in the 4+4 phase, for $\gamma_4 > 0$, $\gamma_6 > 0$. All eight field components have a nonvanishing expectation value of identical magnitude. This phase has an enlarged unit cell of $4 \times 4 \times 4 = 64$, in a fcc Bravais lattice.

Here we follow Balents *et al.*,[1,2] who generalized the calculations of Halperin, Lubensky, and Ma[31] and Brezin *et al.*,[32] and consider a general q-component [U(1)] action

$$\mathcal{S}_0 = \int d^D r \left(\sum_{\ell=0}^{q-1} |(\partial_\mu - i\alpha_\mu)\varphi_\ell|^2 + s|\varphi_\ell|^2 + \frac{1}{2e^2} F^2 \right),$$

$$\mathcal{S}_1 = \frac{1}{4} \int d^D r \sum_{\ell,m,n,i=0}^{q-1} u_{\ell m;ni} \varphi_\ell^* \varphi_m^* \varphi_n \varphi_i. \tag{63}$$

Here we have written the theory for a general space-time dimensionality D. For the quantum critical point of interest, $D=3+1=4$ total space-time dimensions. For this very general action the RG flows obtained by an ϵ expansion are[1,2]

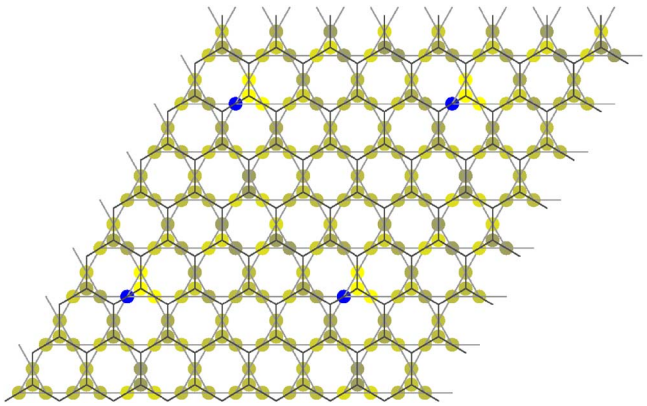

FIG. 17. (Color online) The spin density variations in the 4+4 phase, for $\gamma_4 < 0$, $\gamma_6 > 0$. All eight field components have a nonvanishing expectation value of identical magnitude. This phase has an enlarged unit cell of $4 \times 4 \times 4 = 64$, in a fcc Bravais lattice.

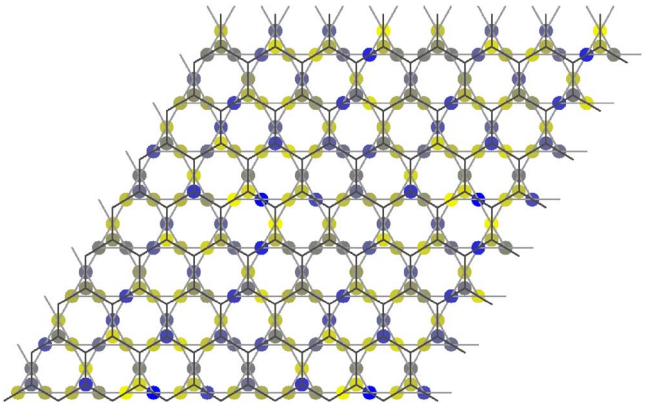

FIG. 18. (Color online) The spin density variations in the 4+4 phase, for $\gamma_4>0$, $\gamma_6<0$. All eight field components have a nonvanishing expectation value of identical magnitude. This phase has an enlarged unit cell of $4\times4\times4=64$, in a fcc Bravais lattice.

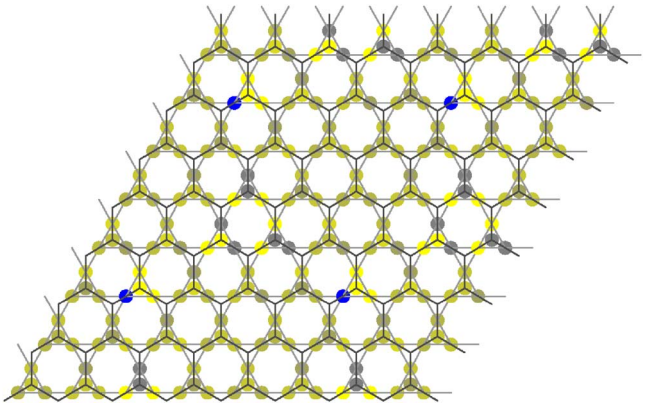

FIG. 19. (Color online) The spin density variations in the 4+4 phase, for $\gamma_4<0$, $\gamma_6<0$. All eight field components have a nonvanishing expectation value of identical magnitude. This phase has an enlarged unit cell of $4\times4\times4=64$, in a fcc Bravais lattice.

$$\frac{de^2}{d\ell} = \epsilon e^2 - \frac{Cq}{3}e^4,$$

$$\frac{du_{\ell m;nk}}{d\ell} = (\epsilon + 2\eta)u_{\ell m;nk} - a_2 e^4 C(\delta_{\ell n}\delta_{mk} + \delta_{\ell k}\delta_{mn}) - C\sum_{ij}\left(\frac{1}{2}u_{\ell m;ij}u_{ij;nk} + u_{\ell i;nj}u_{mj;ki} + u_{\ell i;kj}u_{mj;ni}\right),$$

$$\eta = a_1 e^2 C, \tag{64}$$

with *spatial* dimension $d=3-\epsilon$. Here $\eta=a_1e^2C$ is the anomalous dimension of the fields. The constants $C, a_{1,2}$ were calculated[1,2] in an ϵ expansion. For our case $\epsilon=0$ since our model is in 3+1 space-time dimensions. Thus the ϵ expansion results hold exactly: $C=1/8\pi^2$, $a_1=3$, $a_2=6$.

We take directly $\varphi\to\zeta,\xi$ in the action (42) to make contact with the couplings γ_j

$$u_{mm;mm} = 4\gamma_1,$$

$$u_{mn;mn} = 4\left(\gamma_2 + \frac{1}{2}\gamma_1\right), \quad n\neq m,$$

$$u_{m\bar{n};m\bar{n}} = (\gamma_3 + 2\gamma_1),$$

$$u_{a\bar{b};c\bar{d}} = \gamma_4 \kappa_{a\bar{b}}^{\ c\bar{d}}, \quad a\neq c, \quad b\neq d, \tag{65}$$

where the indices $\in 0,\ldots,3$ and the indices with overbars denote the ξ_j quartet of field components. All other u_{ijkl} couplings vanish in our special case. This "structure" encodes in it the specific symmetry group of our lattice model. Therefore, the RG flow equations should preserve this general structure—only four independent couplings, and the κ tensor must retain its structure. This provides a good check that we have indeed included all possible quartic terms allowed by the symmetry of the problem.

Some manipulation gives us the flow equations for our four couplings:

$$\frac{d\gamma_1}{d\ell} = -C(3e^4 - 6e^2\gamma_1 + 8\gamma_1^2 + 16\gamma_1\gamma_2 + 16\gamma_2^2 + 8\gamma_1\gamma_3 + 2\gamma_3^2),$$

$$\frac{d\gamma_2}{d\ell} = C(6e^2\gamma_2 - 2\gamma_1\gamma_2 + 2\gamma_2^2 - \gamma_4^2),$$

$$\frac{d\gamma_3}{d\ell} = 2C(16\gamma_2^2 + 3e^2\gamma_3 - 6\gamma_1\gamma_3 - 8\gamma_2\gamma_3 + \gamma_3^2 - 3\gamma_4^2),$$

$$\frac{d\gamma_4}{d\ell} = 2C(3e^2 - 6\gamma_1 - 2\gamma_3 - \gamma_4)\gamma_4. \tag{66}$$

The only fixed point allowed by the RG equations is a trivial fixed point with all coupling strengths vanishing $\gamma_i=0$, $e=0$.

The stability or lack thereof of such coupled nonlinear differential equations is not obvious. We would like to know if there is a subspace of codimension zero of the four-dimensional phase space (we may project it onto the $e=0$ plane since the evolution $e>0$ is clearly monotonically decreasing toward zero) in which all couplings scale toward zero. While we have not been able to prove this is not the case, our numerical and analytical investigations have found no such stable regime. We did find a few specific fine-tuned stable solutions, but these were all unstable to infinitesimal perturbations. Thus we believe that the mean-field critical behavior is always destabilized by fluctuations. We expect this probably signals a fluctuation-driven weakly first-order transition. Intuitively, this is a result of the gauge field fluctuations,[31] which lead to attractive interactions amongst the monopoles, driving bound state formation. Note that this result is reliable only for the zero-temperature transition with $D=3+1=4$, the upper critical dimension, where the perturbative renormalization group treatment is justified. In $D=3+0$, the same field theory may well have nontrivial stable (if one parameter is tuned to criticality) fixed points. We will return to this point in the discussion below.

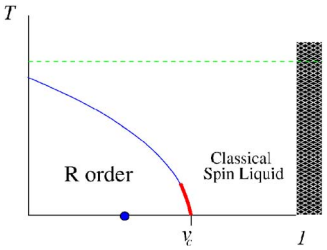

FIG. 20. (Color online) Schematic phase diagram of the spin-dimer model in the $v-T$ plane. At zero temperature, we suppose there is a direct transition from a U(1) spin liquid to the R state at $v=v_c<1$. The thick (red online) portion of the $T>0$ phase boundary is first order, while the thin (blue online) boundary denotes a possible nontrivial "non-LGW" second-order transition at higher temperature.

VIII. DISCUSSION

In the preceding sections, we have presented a systematic study of the zero temperature ordered phases proximate to a "half-polarized" (from the 3:1 constraint) U(1) spin liquid on the pyrochlore lattice, based on a projective symmetry group analysis of the monopole excitations of the liquid state. One of these states would be expected to occur on reducing v in the spin and dimer model starting from a value ($\lesssim 1$) within the spin liquid state. The ordered phases, determined at the mean-field level, all break discrete symmetries of the pyrochlore lattice, and in particular we find a generic unit cell enlargement, with the minimal cell size four times that of the underlying pyrochlore lattice, and a maximal unit cell 64 times larger. The simplest R state, with the smallest unit cell, is the same one which was found to be the ground state in the "classical" spin or dimer limit $v\to-\infty$. It therefore seems likely that the spin and dimer model exhibits only two phases for $v<1$, and hence a *direct* quantum phase transition from the U(1) spin liquid to the R state. If this is indeed the case, one may contemplate the possibility that $HgCr_2O_4$ (or other pyrochlore chromates) might be close to this quantum critical point.

While previous work[13] and the main text has focused almost entirely upon the ground state properties of the spin and dimer model, it is interesting to consider the more general problem at nonzero temperature $T>0$. A schematic phase diagram in the $v-T$ plane is illustrated in Fig. 20. We will focus on the region $v<1$, and will not discuss the physics of the thermal ensemble of "frozen" states occuring for $v>1$. First, we note that the R state has a gap to all excitations, and breaks only discrete lattice symmetries. We therefore expect that the R state will persist at $T>0$ up to some nonzero critical temperature $T_c(v)>0$ for $v<v_c$. By contrast, the U(1) quantum spin liquid ground state breaks no symmetries. Therefore, in the dimer model, no transition is expected for $v_c<v<1$ as T is increased from zero to infinity. We thus expect just the single phase boundary emanating from the quantum critical point, shown in Fig. 20.

It might appear from these observations that the *thermal* ordering transition at $T_c(v)$ should be a rather ordinary one, described by the usual Landau-Ginzburg-Wilson (LGW) approach based on the order parameter of the R state. In fact this is incorrect, and $T>0$ problem is rather more interesting. To see this, let us consider the "paramagnetic" state obtained for very high temperature in the dimer model. The physics of such classical, infinite-temperature dimer models (and other similarly constrained models) have been considered by several authors.[6,22,28] As shown in these works, due to the dimer constraint, even at infinite temperature the dimer model has nontrivial power-law "dipolar" correlations. Such dipolar correlations are not captured by the conventional LGW theory which retains only the order parameter.

To understand these dipolar correlations, and a proper formulation of the phase transition in the spin-dimer model, it is instructive to return to the monopole field theory in Eq. (63). Let us rewrite this effective action making space and time coordinates separate and explicit:

$$\mathcal{S}_0=\int d^3r\int_0^\beta d\tau\left(\sum_{\ell=0}^{q-1}|(\partial_\tau-i\alpha_0)\varphi_\ell|^2+|(\vec{\nabla}-i\vec{\alpha})\varphi_\ell|^2+s|\varphi_\ell|^2+\frac{1}{2e^2}(\partial_\tau\vec{\alpha}-\vec{\nabla}\alpha_0)^2+\frac{1}{2e^2}(\vec{\nabla}\times\vec{\alpha})^2\right),$$

$$\mathcal{S}_1=\frac{1}{4}\int d^3r\int_0^\beta d\tau\sum_{\ell,m,n,i=0}^{q-1}u_{\ell m;ni}\varphi_\ell^*\varphi_m^*\varphi_n\varphi_i. \qquad (67)$$

Here $\beta=(k_BT)^{-1}$ is the inverse temperature. To derive a theory of the thermal phase transition at $T>0$, we use standard logic to proceed from Eq. (67). In particular, at $T>0$, imposing periodic boundary conditions (as demanded by the trace defining the quantum statistical mechanical partition function) in imaginary time leads to a set of discrete bosonic Matsubara frequencies $\omega_n=2\pi n/\beta$, with integer n. Because of the time-derivative term, all modes with $\omega_n\neq 0$ have enhanced "masses" relative to the zero Matsubara frequency mode, and can be integrated out. Practically speaking, this amounts to assuming the order parameter is constant in imaginary time, $\partial_\tau\varphi_\ell=0$. Similarly, we may take $\partial_\tau\vec{\alpha}=0$, and by a choice of gauge, $\alpha_0=0$. Carrying out this procedure, we find $\mathcal{S}_0+\mathcal{S}_1=\mathcal{F}/k_BT$, where $\mathcal{F}=\mathcal{F}_0+\mathcal{F}_1$ is an effective classical free energy:

$$\mathcal{F}_0=\int d^3r\left(\sum_{\ell=0}^{q-1}|(\vec{\nabla}-i\vec{\alpha})\varphi_\ell|^2+s|\varphi_\ell|^2+\frac{1}{2e^2}(\vec{\nabla}\times\vec{\alpha})^2\right),$$

$$\mathcal{F}_1=\frac{1}{4}\int d^3r\sum_{\ell,m,n,i=0}^{q-1}u_{\ell m;ni}\varphi_\ell^*\varphi_m^*\varphi_n\varphi_i. \qquad (68)$$

Equation (68) is precisely the classical "Ginzburg-Landau" free energy for a multicomponent superconductor in three dimensions, with the quartic interaction $u_{\ell m;ni}$ determined by the PSG. The interpretation of this result is quite simple. In the U(1) spin liquid, the monopole is a well-defined, bosonic particle excitation, and carries the "magnetic" gauge charge. The magnetic gauge charge is conserved in the theory. As already discussed, the ordered (R) state at zero temperature is understood as a condensate of these monopoles. In fact, within the quantum dimer model, the bosonic monopole can condense at a nonzero tempera-

ture, just as in an ordinary Bose-Einstein condensate. Thus Eq. (68) is nothing but the "classical" free energy describing the "superfluid" transition of this monopole. Because it carries a nonzero magnetic gauge charge, it is coupled to the electric vector potential $\vec{\alpha}$, just as the electric charged Cooper pair condensate is coupled to the magnetic vector potential in ordinary superconductivity.

Thus we are led to this remarkable and unconventional description of the $T>0$ phase transition between the paramagnet and the R state. Without the 3:1 spin-dimer constraint, this transition would certainly be expected to be governed by conventional Landau theory. What is the nature of the unconventional transition? According to the $d=4-\epsilon$ expansion approach (discussed in Sec. VII), this transition is fluctuation-driven first order. However, this conclusion is known to be often incorrect for the physical case of Ginzburg-Landau transitions in three dimensions. In particular, a class of related models, N-component Ginzburg-Landau theories with U(N) symmetry, have been investigated in a number of cases. First, for sufficiently large N, these transitions can be shown to be second order in an expansion around $N=\infty$. Second, for $N=1$, a duality transformation has been used to demonstrate that the transition can be continuous, in the inverted XY universality class.[33] A similar duality analysis, in conjunction with numerics, has been used in arguing for continuous critical behavior for $N=2$.[34] It therefore appears quite likely that continuous critical behavior is possible in these models for *any* N. By analogy, continuous critical behavior of the theory of Eq. (68) seems quite possible. We thus suggest that the paramagnetic to R state transition in the spin-dimer model constitutes a non-LGW universality class. Note that, since the RG analysis in Sec. VII concluded that the $T=0$ quantum phase transition is weakly first order, the phase boundary for *very* small but nonzero temperature must remain discontinuous. We therefore expect a multicritical point separating on the $T>0$ phase boundary separating first order from continuous non-LGW critical behavior. The continuous and first order portions of the phase boundary are shown in Fig. 20 by thin (blue online) and thick (red online) lines, respectively. It would be of considerable interest to investigate this classical phase transition in the the spin-dimer model numerically. This could be done on a purely classical dimer model, with $K=0$, and so would require only classical Monte Carlo methods.

As remarked above, without the 3:1 spin-dimer constraint, the classical phase transition would certainly be expected to be described by LGW theory. For any microscopic model, such as the spin-3/2 Heisenberg model of Ref. 13, the 3:1 constraint is not expected to be exactly obeyed. At zero temperature, however, pyrochlore tetrahedra violating the 3:1 constraint are gapped excitations, and are not present in the ground state on the plateau. Consider configurations in which a single tetrahedron violates the constraint by having either zero or two minority spins instead of one. In the mapping to the gauge theory, these particular excitations can be viewed as states with "electric" gauge charge ± 1 (relative to the static background gauge charge of the plateau states) on the tetrahedron in question. They also carry physical spin $\Delta S^z = \pm 3/2$ relative to the plateau states. This follows because the total spin can be written as

$$S^z_{\rm tot} = \frac{1}{2}\sum_t S^z_t, \tag{69}$$

the factor of 1/2 being required since each spin is contained in two tetrahedra. These excited states can therefore be viewed as fractional spin excitations, or "spinons," in this particular example. In any case, because they cost only finite energy, there will be a non-vanishing concentration of such electric gauge charges at $T>0$, due to thermal activation. The typical separation of the electric gauge charges is expected to behave exponentially at low temperature, $\lambda \sim \exp(\Delta/k_B T)$, if Δ is the gap to the electric charged particles. This has several effects. First, the dipolar correlations of the paramagnetic phase of the spin-dimer model will cross over to the usual exponential ones of an ordinary paramagnet, for lengths larger than λ. Moreover, the "plasma" of electric charges is expected to give rise to a linear confining potential between oppositely (magnetically) charged monopoles. This will bind the monopoles and antimonopoles into gauge-neutral pairs, the radius of this bound state being at least as large as λ. It is only these pairs that can Bose condense. When λ is large, there is a crossover behavior. On approaching the paramagnetic to R state transition, the correlation length grows in a manner first governed by the non-LGW theory of Eq. (68). Once the correlation length exceeds the monopole-antimonopole binding length, these pairs may be considered well formed, and the critical behavior changes to that described by Bose condensation of the pairs. The creation and annihilation operators for the monopole-antimonopole bound states are expected to be proportional to

$$\Psi_{\ell\ell'} \sim \varphi^*_\ell \varphi_{\ell'}. \tag{70}$$

Since φ^*_ℓ and φ_ℓ transform under conjugate representations of the PSG, and hence $\Psi_{\ell\ell'}$ is gauge neutral, it transforms not under the PSG but simply the ordinary lattice space group. Hence $\Psi_{\ell\ell'}$ can be decomposed into irreducible representations of the space group, which are precisely the usual Landau order parameters. Thus the critical behavior sufficiently close to the phase boundary, when the 3:1 spin-dimer constraint is not rigidly enforced, is indeed governed by LGW theory as expected on general grounds. The conventional LGW analysis is straightforward, and will be presented in Ref. 35. It predicts that the paramagnetic to R state transition should be first order, due to the presence of a cubic invariant. For $k_B T \ll \Delta$, it will be weakly so along the thin (blue) portion of the phase boundary in Fig. 20. Of course there is no such crossover in the spin-dimer model, for which the constraint is rigidly enforced.

In summary, we have studied the phase structure of a spin-dimer model on the pyrochlore or diamond lattice. It contains an interesting quantum paramagnetic "U(1) spin liquid" phase at zero temperature, as well as an ordered R state at $T \geqslant 0$. We derived a novel monopole field theory to describe the quantum and classical phase transitions between the quantum and classical paramagnets and the R state. Prior work in Ref. 13 indicates that the half-polarized magnetization plateau of the spin-3/2 Heisenberg antiferromagnet on the pyrochlore lattice is described by this model, with a cou-

pling constant that places it in the R state at low temperature. It is interesting to contemplate the possibility that the experimental materials $CdCr_2O_4$ and $HgCr_2O_4$ might be near the quantum phase transition of the paper to the spin liquid state. It would indeed be exciting were some homologous material to actually realize the U(1) spin liquid in its plateau ground state. To this end, we note that, were a spin-1/2 pyrochlore antiferromagnet to be realized experimentally, the quantum effects would be significantly further increased, and a U(1) spin liquid might well be expected theoretically. We leave such tantalizing possibilities as open questions.

ACKNOWLEDGMENTS

We are grateful to A. A. Burkov, M. Hermele, O. I. Motrunich, and R. Shindou for enlightening discussions. This work was generously supported by NSF Grants No. DMR04-57440 and No. PHY99-07949, and the Packard Foundation.

APPENDIX A: GROUND STATE EIGENMODES

The diamond lattice is bipartite and can be thought of as being made of two fcc sub-lattices one shifted from the other by the vector $\vec{b}=-\frac{1}{4}(\vec{a}_1+\vec{a}_2+\vec{a}_3)$ where $\vec{a}_j$ are the fcc primitive vectors. We introduce the notation

$$\eta_1(\vec{n}) = \psi(\vec{r}), \quad \eta_2(\vec{n}) = \psi(\vec{r}+\vec{b}), \tag{A1}$$

where $\vec{r}$ denotes sites on a fcc lattice, $\vec{r}+\vec{b}$ are the sites of the second fcc lattice comprising the diamond lattice, and $\vec{n}$ are the "index" space coordinates on the fcc lattice.

Defining the Fourier transform of the wave function η, and its inverse as

$$\eta(\vec{n}) = \int_{\vec{k}\in BZ} \frac{d^3\vec{k}}{(2\pi)^3}\eta(\vec{k})\cdot e^{+i\vec{k}\cdot\vec{n}},$$

$$\eta(\vec{k}) = \sum_{\vec{n}} e^{-i\vec{k}\cdot\vec{n}}\cdot\eta(\vec{n}), \tag{A2}$$

we can write out the eigenstates in a compact manner

$$\Phi_\nu = \sum_{\substack{\mu=0\ldots3\\ a=1,2}} c_\mu^{(a)}\eta_a(\vec{p}_{\mu,\nu})e^{-i(\pi/2)\mu\nu},$$

$$\bar{\Phi}_\nu = \sum_{\substack{\mu=0\ldots3\\ a=1,2}} c_{-\mu}^{(\bar{a})}\eta_a(\vec{q}_{\mu,\nu})e^{-i(\pi/2)\mu\nu}, \tag{A3}$$

where $|0\rangle$ denotes the vacuum state, and

$$\vec{p}_{\mu,\nu} = \vec{p} + \mu\vec{Q} + \frac{\pi}{2}\nu\vec{\epsilon},$$

$$\vec{q}_{\mu,\nu} = \vec{d} - \vec{p} + \mu\vec{Q} + \frac{\pi}{2}\nu\vec{\epsilon}, \tag{A4}$$

where $\vec{p}=(\pi/2,\pi/4,\pi/4)$ and $\vec{d}=(\pi/2,0,\pi)$. The coefficients are

$$c_{\mu,\nu}^{(a)} = c_\mu^{(a)}e^{-i(\pi/2)\mu\nu}, \tag{A5}$$

where $c_\mu^{(a)}=c_{\mu,0}^{(a)}$ are the coefficients for the $\nu=0$ state. Finally, the unnormalized coefficients $c_\mu^{(a)}$ are

$$c_\mu^{(1)} = \left(1,-i,\frac{-i}{1+\sqrt{2}},\frac{1}{1+\sqrt{2}}\right),$$

$$c_\mu^{(2)} = \left(\frac{3-i}{\sqrt{10}},\frac{1-2i}{\sqrt{5}+\sqrt{10}},-\frac{1+3i}{\sqrt{10}(1+\sqrt{2})},\frac{2+i}{\sqrt{5}}\right). \tag{A6}$$

APPENDIX B: PROJECTIVE SYMMETRY GROUP

We start by enumerating some diamond lattice symmetries. Since the diamond lattice is made up of two fcc lattices, it inherits the translations of the fcc lattice

$$\hat{t}_j:\vec{r}\to\vec{r}+\vec{a}_j. \tag{B1}$$

Next we consider a threefold rotation symmetry

$$r_3:(x,y,z)\to(z,x,y), \tag{B2}$$

and a twofold rotation

$$r_2:(x,y,z)\to(x,-y,-z). \tag{B3}$$

There is also a reflection symmetry

$$i:(x,y,z)\to(x,z,y). \tag{B4}$$

Finally we have an inversion symmetry that effectively swaps between the two fcc sublattices

$$p:\vec{r}\to\vec{b}-\vec{r}. \tag{B5}$$

To construct the PSG we attach gauge transformations to each symmetry operation. This is most easily done in the index space coordinates, and we now list the action of the PSG operations on the wave functions. First are the three lattice translations

$$\hat{T}_j:\eta(\vec{n})\to\eta(\vec{n}+\vec{a}_j)e^{-i\Lambda_j(\vec{n})}, \tag{B6}$$

where

$$\Lambda_j(\vec{n}) = -(\vec{\epsilon}\cdot\vec{n})Q_j. \tag{B7}$$

The inversion symmetry

$$\hat{\mathcal{P}}:\eta(\vec{n})\to\hat{\sigma}_x\cdot\eta(-\vec{n})e^{-i\Lambda_C(\vec{n})}, \tag{B8}$$

where σ_x is the x Pauli matrix, and

$$\Lambda_C(\vec{n}) = -\vec{d}\cdot\vec{n} = -\frac{\pi}{2}(1,0,-2)\cdot\vec{n}. \tag{B9}$$

The threefold rotation

$$\hat{\mathcal{R}}_{(3)}:\eta(\vec{n})\to\eta(\hat{\mathcal{R}}_{(3)}\cdot\vec{n})e^{-i\Lambda_{\mathcal{R}_3}(\vec{n})}, \tag{B10}$$

with the gauge transformation

$$\Lambda_{\mathcal{R}_3}(\vec{n}) = \vec{n}\cdot\hat{B}_1\cdot\vec{n} + \vec{\delta}\cdot\vec{n}, \tag{B11}$$

where

$$\hat{B}_1 = \frac{\pi}{4}, \quad \begin{pmatrix} 1 & 1 & 2 \\ 1 & 2 & 1 \\ 2 & 1 & 1 \end{pmatrix}, \quad \vec{\delta} = -\frac{\pi}{4}(1,2,1). \tag{B12}$$

The twofold rotation

$$\hat{\mathcal{R}}_{(2)}: \begin{cases} \eta_1(\vec{n}) \to \eta_1(\hat{\mathcal{R}}_{(2)} \cdot \vec{n}) e^{-i\Lambda^{(1)}_{\mathcal{R}_2}(\vec{n})}, \\ \eta_2(\vec{n}) \to \eta_2(\hat{\mathcal{R}}_{(2)} \cdot \vec{n} + \vec{a}_1) e^{-i\Lambda^{(2)}_{\mathcal{R}_2}(\vec{n})}. \end{cases} \tag{B13}$$

The gauge transformations for the two spinor components are different,

$$\Lambda^{(1)}_{\mathcal{R}_2}(\vec{n}) = \vec{n} \cdot \hat{B}_2 \cdot \vec{n} + \vec{\lambda}_1 \cdot \vec{n}, \tag{B14a}$$

$$\Lambda^{(2)}_{\mathcal{R}_2}(\vec{n}) = \vec{n} \cdot \hat{B}_2 \cdot \vec{n} + \vec{\lambda}_2 \cdot \vec{n}, \tag{B14b}$$

where

$$\hat{B}_2 = \frac{\pi}{2} \begin{pmatrix} 0 & 1 & 1 \\ 1 & 1 & 0 \\ 1 & 0 & 1 \end{pmatrix}, \tag{B15}$$

and

$$\vec{\lambda}_1 = \frac{\pi}{2}(-1,1,2), \quad \vec{\lambda}_2 = \vec{\lambda}_1 + \frac{\pi}{2}(1,2,1). \tag{B16}$$

Finally, the reflection symmetry

$$\hat{\mathcal{I}}: \eta(\vec{n}) \to \eta^\dagger(\hat{\mathcal{I}} \cdot \vec{n}) e^{-i\Lambda_{\hat{\mathcal{I}}}(\vec{n})}, \tag{B17}$$

and the gauge transformation is

$$\Lambda_{\hat{\mathcal{I}}}(\vec{n}) = \vec{n} \cdot \hat{B}_3 \cdot \vec{n} + \vec{\xi} \cdot \vec{n}, \tag{B18}$$

where

$$\hat{B}_3 = -\frac{\pi}{4} \begin{pmatrix} 2 & 1 & 1 \\ 1 & 2 & 1 \\ 1 & 1 & 2 \end{pmatrix}, \quad \vec{\xi} = \frac{\pi}{2}(1,1,1). \tag{B19}$$

One can take the Fourier transform of these symmetry operations, to find their action on $\eta(\vec{k})$ and then deduce how the eight ground state eigenmodes transform under them. The transformation rules (D1)–(D6) are the result of that analysis. It is a good check that the ground state manifold is invariant under every one of these symmetries. Although the ground state manifold need not be completely connected by the symmetry operations, in our case it is.

APPENDIX C: GROUP ALGEBRA

The diamond lattice symmetry group, described by the reduced set of operations introduced in the text, obeys the algebra

$$r_3{}^3 = 1, \quad r_2{}^2 = 1, \quad p^2 = 1, \quad i^2 = 1,$$

$$r_3 \cdot p \cdot r_3{}^{-1} \cdot p = 1, \quad t_i \cdot t_j \cdot t_i{}^{-1} \cdot t_j{}^{-1} = 1,$$

$$(p \cdot t_j)^2 = 1, \quad r_3 \cdot t_j \cdot r_3{}^{-1} \cdot t_{j+1}{}^{-1} = 1,$$

$$r_2 \cdot t_1 \cdot r_2 \cdot t_1 = 1, \quad r_2 \cdot t_2 \cdot r_2 \cdot t_1 = t_3, \quad r_2 \cdot t_3 \cdot r_2 \cdot t_1 = t_2,$$

$$i \cdot t_1 = t_1 \cdot i, \quad i \cdot t_2 = t_3 \cdot i, \quad i \cdot t_3 = t_2 \cdot i,$$

$$i \cdot r_3 = r_3{}^{-1} \cdot i, \quad i \cdot r_2 = r_2 \cdot i, \quad i \cdot p = p \cdot i. \tag{C1}$$

APPENDIX D: GROUND STATE MANIFOLD PERMUTATIVE REPRESENTATION OF PSG

In the basis of (38) the PSG realizes a permutative representation,[1] i.e. each generator can be written as $G = \Lambda(G)P(G)$, where $\Lambda(G)$ is a diagonal matrix with unimodular complex entries, and $P(G)$ is a permutation matrix, acting on the eight-component vector $(\vec{\zeta}, \vec{\xi})$. One finds:

$$\Lambda(\hat{T}_1) = \mathrm{diag}(i,i,1,-1,1,1,-i,i),$$

$$P(\hat{T}_1) = (43218765), \tag{D1}$$

$$\Lambda(\hat{T}_2) = \mathrm{diag}(z,z,iz,iz,-iz,-iz,z,z),$$

$$P(\hat{T}_2) = (21436587), \tag{D2}$$

$$\Lambda(\hat{\mathcal{R}}_{(2)}) = \mathrm{diag}(z^*,z,-z^*,-z,z,z^*,z^*,z),$$

$$P(\hat{\mathcal{R}}_{(2)}) = (21437856), \tag{D3}$$

$$\Lambda(\hat{\mathcal{R}}_{(3)}) = \mathrm{diag}(z,1,-z^*,-1,z,1,z^*,1),$$

$$P(\hat{\mathcal{R}}_{(3)}) = (32417685), \tag{D4}$$

$$\Lambda(\hat{\mathcal{P}}) = \mathrm{diag}(1,1,1,-1,1,1,1,-1),$$

$$P(\hat{\mathcal{P}}) = (56781234), \tag{D5}$$

$$\Lambda(\hat{\mathcal{I}}) = \mathrm{diag}(w,w,iw,-w,-w,w,iw,w),$$

$$P(\hat{\mathcal{I}}) = (86754231). \tag{D6}$$

Here $z = e^{i\pi/4}$, $w = (1-2i)/\sqrt{5}$, diag$(\cdot)$ is the diagonal matrix with entries $\cdot$, and permutations are specified in the standard way by the result of permuting the integers 1, …, 8. Finally, $\hat{\mathcal{I}}$ should be understood as acting after complex conjugation of the monopole field vector

$$\hat{\mathcal{I}}: (\vec{\zeta}, \vec{\xi}) \to \Lambda(\hat{\mathcal{I}}) P(\hat{\mathcal{I}}) (\vec{\zeta}^*, \vec{\xi}^*). \tag{D7}$$

APPENDIX E: κ TENSOR

The κ [in Eq. (40)] tensor was hiding the following expression:

$$\Theta_4 = \sum_{ijkl} \kappa_{ij}^{kl} \zeta_k \xi_l \zeta_i^* \xi_j^* = \zeta_1 \xi_1 \zeta_0^* \xi_0^* + \zeta_2 \xi_2 \zeta_0^* \xi_0^* + i\zeta_3 \xi_3 \zeta_0^* \xi_0^*$$
$$- \zeta_0 \xi_1 \zeta_1^* \xi_0^* + i\zeta_3 \xi_2 \zeta_1^* \xi_0^* + \zeta_2 \xi_3 \zeta_1^* \xi_0^* - \zeta_3 \xi_1 \zeta_2^* \xi_0^*$$
$$+ \zeta_0 \xi_2 \zeta_2^* \xi_0^* + i\zeta_1 \xi_3 \zeta_2^* \xi_0^* - \zeta_2 \xi_1 \zeta_3^* \xi_0^* + i\zeta_1 \xi_2 \zeta_3^* \xi_0^*$$
$$- \zeta_0 \xi_3 \zeta_3^* \xi_0^* - \zeta_1 \xi_0 \zeta_0^* \xi_1^* - \zeta_3 \xi_2 \zeta_0^* \xi_1^* - i\zeta_2 \xi_3 \zeta_0^* \xi_1^*$$
$$+ \zeta_0 \xi_0 \zeta_1^* \xi_1^* - i\zeta_2 \xi_2 \zeta_1^* \xi_1^* - \zeta_3 \xi_3 \zeta_1^* \xi_1^* - \zeta_3 \xi_0 \zeta_2^* \xi_1^*$$
$$- \zeta_1 \xi_2 \zeta_2^* \xi_1^* + i\zeta_0 \xi_3 \zeta_2^* \xi_1^* - \zeta_2 \xi_0 \zeta_3^* \xi_1^* + i\zeta_0 \xi_2 \zeta_3^* \xi_1^*$$
$$+ \zeta_1 \xi_3 \zeta_3^* \xi_1^* + \zeta_2 \xi_0 \zeta_0^* \xi_2^* - i\zeta_3 \xi_1 \zeta_0^* \xi_2^* + \zeta_1 \xi_3 \zeta_0^* \xi_2^*$$
$$- i\zeta_3 \xi_0 \zeta_1^* \xi_2^* - \zeta_2 \xi_1 \zeta_1^* \xi_2^* + \zeta_0 \xi_3 \zeta_1^* \xi_2^* + \zeta_0 \xi_0 \zeta_2^* \xi_2^*$$
$$+ i\zeta_1 \xi_1 \zeta_2^* \xi_2^* + \zeta_3 \xi_3 \zeta_2^* \xi_2^* - i\zeta_1 \xi_0 \zeta_3^* \xi_2^* - \zeta_0 \xi_1 \zeta_3^* \xi_2^*$$
$$- \zeta_2 \xi_3 \zeta_3^* \xi_2^* - \zeta_3 \xi_0 \zeta_0^* \xi_3^* - i\zeta_2 \xi_1 \zeta_0^* \xi_3^* + \zeta_1 \xi_2 \zeta_0^* \xi_3^*$$
$$- i\zeta_2 \xi_0 \zeta_1^* \xi_3^* + \zeta_3 \xi_1 \zeta_1^* \xi_3^* + \zeta_0 \xi_2 \zeta_1^* \xi_3^* + \zeta_1 \xi_0 \zeta_2^* \xi_3^*$$
$$+ i\zeta_0 \xi_1 \zeta_2^* \xi_3^* - \zeta_3 \xi_2 \zeta_2^* \xi_3^* - i\zeta_0 \xi_0 \zeta_3^* \xi_3^*$$
$$- \zeta_1 \xi_1 \zeta_3^* \xi_3^* + \zeta_2 \xi_2 \zeta_3^* \xi_3^*. \quad \text{(E1)}$$

APPENDIX F: PROOF THAT THE LOWEST DIMENSION OF A REPRESENTATION OF THE PSG IS 8

We start by assuming that we are in a basis where $\hat{T}_1$ is diagonal. Denote one eigenvector by

$$\hat{T}_1 \psi_0 = \lambda \psi_0. \quad \text{(F1)}$$

The PSG algebra rule (36) dictates that $\hat{T}_2$ cannot be diagonal in this basis. Using

$$\hat{T}_2 \cdot \hat{T}_1 = \hat{T}_1 \cdot \hat{T}_2(-i), \quad \text{(F2)}$$

we find ψ_0 is connected to a four-cycle of eigenvectors

$$\psi_m = \hat{T}_2^m \psi_0, \quad \text{(F3)}$$

with eigenvalues

$$\hat{T}_1 \psi_m = \lambda i^m \psi_m. \quad \text{(F4)}$$

This proves that the translations must all be constructed only of four-cycles. As a consequence, any representation of the PSG can only be of a dimension $d = 4 \times n$.

We know already that an eight-dimensional representation (rep) exists (D1)–(D6), so we need only consider the $d=4$ case, and show that it is impossible.

Assume we have a $d=4$ rep. Therefore, each eigenvalue is nondegenerate, with a unique eigenvector. From (C1) we know that the inversion and $\hat{T}_1$ commute. It is easy to show that

$$(\hat{\mathcal{I}}\psi_m)\lambda i^m = \hat{T}_1(\hat{\mathcal{I}}\psi_m) \quad \text{(F5)}$$

follows, and since only a unique eigenvector has this eigenvalue, we conclude that

$$(\hat{\mathcal{I}}\psi_m) = \psi_m \quad \text{(F6)}$$

and that in this rep $\mathcal{I}=1$. From the PSG algebra we now have

$$\hat{\mathcal{I}}\hat{\mathcal{R}}_{(3)} = \hat{\mathcal{R}}_{(3)}^{-1}\hat{\mathcal{I}} \Rightarrow \hat{\mathcal{R}}_{(3)} = \hat{\mathcal{R}}_{(3)}^{-1}. \quad \text{(F7)}$$

The rotation $\mathcal{R}_{(3)}$ is threefold, and therefore in this rep it is also unity. Finally, as $\mathcal{R}_{(3)}=1$ using the rule

$$\hat{T}_2 = \hat{\mathcal{R}}_{(3)}\hat{T}_1\hat{\mathcal{R}}_{(3)}^{-1} \quad \text{(F8)}$$

we find $\hat{T}_1 = \hat{T}_2$, and we have a contradiction.

This contradiction proves a four-dimensional rep of the PSG is not possible, leaving us with $d=8$ as the lowest dimension of a rep of the PSG.

[1] L. Balents, L. Bartosch, A. Burkov, S. Sachdev, and K. Sengupta, Phys. Rev. B **71**, 144508 (2005).
[2] L. Balents, L. Bartosch, A. Burkov, S. Sachdev, and K. Sengupta, Phys. Rev. B **71**, 144509 (2005).
[3] C. Lannert, M. P. A. Fisher, and T. Senthil, Phys. Rev. B **63**, 134510 (2001).
[4] S. Sachdev and K. Park, Ann. Phys. (N.Y.) **298**, 58 (2002).
[5] R. Moessner and J. T. Chalker, Phys. Rev. Lett. **80**, 2929 (1998).
[6] M. Hermele, M. P. A. Fisher, and L. Balents, Phys. Rev. B **69**, 064404 (2004).
[7] P. W. Anderson, Science **235**, 1196 (1987).
[8] X. G. Wen, Phys. Rev. B **65**, 165113 (2002).
[9] R. Moessner and S. L. Sondhi, Phys. Rev. B **68**, 184512 (2003).
[10] D. Foerster, H. B. Nielsen, and M. Ninomiya, Phys. Lett. **94**, 135 (1980).
[11] O. I. Motrunich and T. Senthil, Phys. Rev. B **71**, 125102 (2005).
[12] J.-S. Bernier, Y.-J. Kao, and Y. B. Kim, Phys. Rev. B **71**, 184406 (2005).
[13] D. L. Bergman, R. Shindou, G. A. Fiete, and L. Balents, Phys. Rev. Lett. **96**, 097207 (2006).
[14] H. Ueda, H. A. Katori, H. Mitamura, T. Goto, and H. Takagi, Phys. Rev. Lett. **94**, 047202 (2005).
[15] H. Ueda, H. Mitamura, T. Goto, and H. Takagi (unpublished).
[16] K. Penc, N. Shannon, and H. Shiba, Phys. Rev. Lett. **93**, 197203 (2004).
[17] G. Misguich, D. Serban, and V. Pasquier, Phys. Rev. Lett. **89**, 137202 (2002).
[18] G. Misguich, V. Pasquier, F. Mila, and C. Lhuillier, Phys. Rev. B **71**, 184424 (2005).
[19] A. Ralko, M. Ferrero, F. Becca, D. Ivanov, and F. Mila, Phys. Rev. B **71**, 224109 (2005).
[20] R. Moessner, S. L. Sondhi, and P. Chandra, Phys. Rev. B **64**, 144416 (2001).
[21] R. Moessner and S. L. Sondhi, Phys. Rev. Lett. **86**, 1881 (2001).
[22] D. A. Huse, W. Krauth, R. Moessner, and S. L. Sondhi, Phys. Rev. Lett. **91**, 167004 (2003).
[23] D. S. Rokhsar and S. A. Kivelson, Phys. Rev. Lett. **61**, 2376 (1988).
[24] C. L. Henley, Phys. Rev. Lett. **62**, 2056 (1989).
[25] C. L. Henley, Can. J. Phys. **79**, 1207 (2001).

[26] J. Villain, R. Bidaux, J. Carton, and R. Conte, J. Phys. (France) **41**, 1263 (1980).
[27] J. Kogut, Rev. Mod. Phys. **51**, 659 (1979).
[28] S. V. Isakov, K. Gregor, R. Moessner, and S. L. Sondhi, Phys. Rev. Lett. **93**, 167204 (2004).
[29] L. Balents, L. Bartosch, A. Burkov, S. Sachdev, and K. Sengupta, in Proceedings, Physics of Strongly Correlated Electron Systems YKIS2004 Workshop, Kyoto, Japan, 2004, cond-mat/0504692 (unpublished).
[30] E. Kroumova, M. I. Aroyo, J. M. Perez Mato, A. Kirov, C. Capillas, S. Ivantchev, and H. Wondratschek, Phase Transitions **76**, 155 (2003).
[31] B. I. Halperin, T. C. Lubensky, and S. K. Ma, Phys. Rev. Lett. **32**, 292 (1974).
[32] E. Brézin, J. C. L. Guillou, and J. Zinn-Justin, Phys. Rev. B **10**, 892 (1974).
[33] C. Dasgupta and B. I. Halperin, Phys. Rev. Lett. **47**, 1556 (1981).
[34] O. I. Motrunich and A. Vishwanath, Phys. Rev. B **70**, 075104 (2004).
[35] D. L. Bergman *et al.* (unpublished).
[36] The PSG is useful as a means of classifying emergent gauge structures as discussed by Wen in Ref. 8.